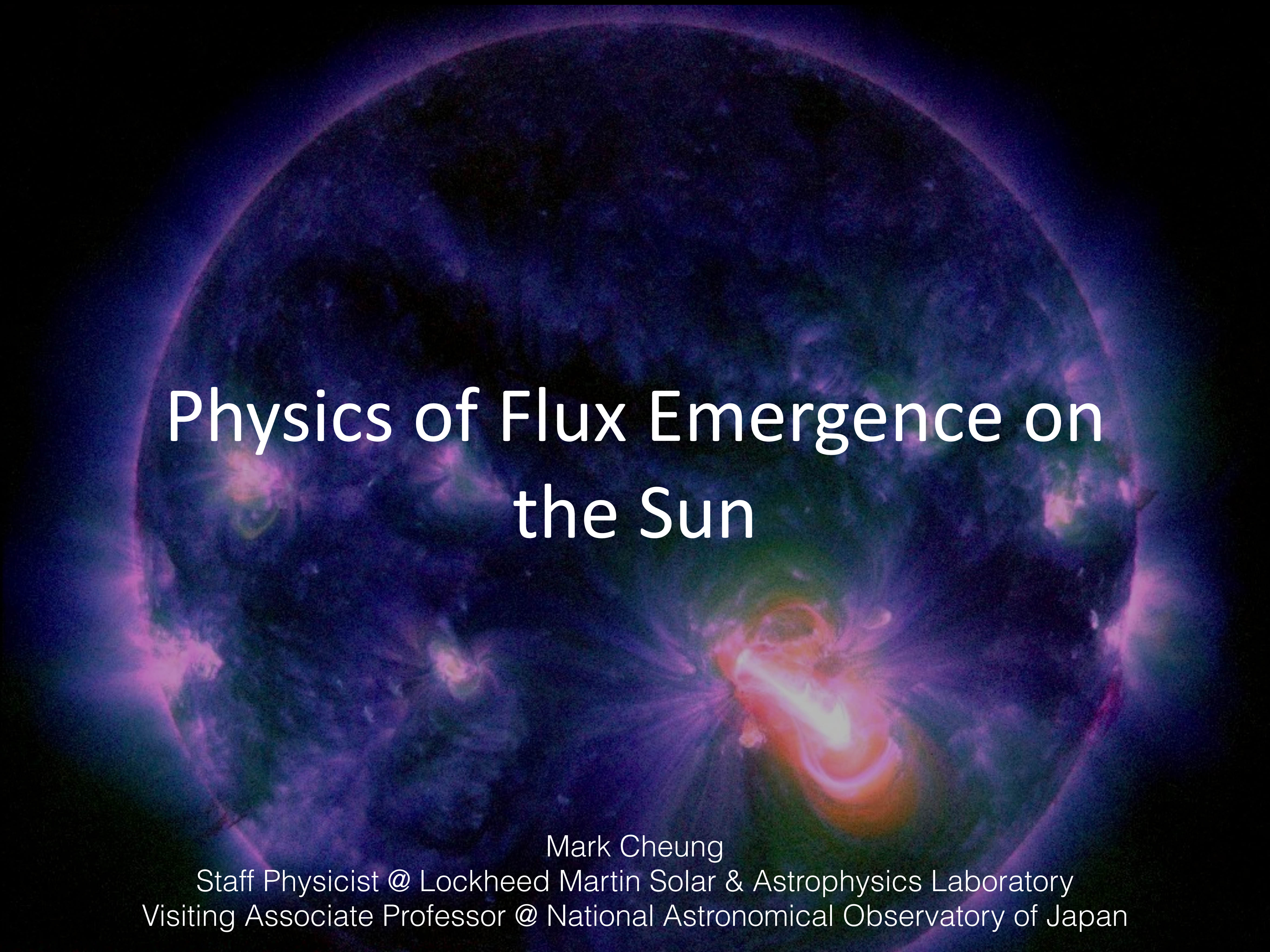

Physics of Flux Emergence on the Sun

Mark Cheung
Staff Physicist @ Lockheed Martin Solar & Astrophysics Laboratory
Visiting Associate Professor @ National Astronomical Observatory of Japan


Eine Familie,
chaft, ein Lang
Lang-Bräu
Läuft.
Lang-Bräu
Lang-Bräu
LIMITED REAL BAYERN BEER FROM GERMANY
限定リアルバイエルンビール&ドイツ最高位マイスターソーセージ
バイエルン・オーバーフランケン最高峰
るドイツ最高位マイスターソーセージ
¥3000
¥2000
¥1100
¥600
¥600
¥600
¥600

Plan

- Lecture I: Physics of Flux Emergence
- Lecture II: Diagnostics of Flux Emergence

Aims of this talk/article

- a primer on the physics that govern the behavior of magnetic fields emerging into the solar atmosphere,

- an introduction of how flux emergence plays a key role in many aspects of solar physics, and

- a broad overview of established and more recent developments in this field of research.

Science questions

- What is the mechanism that brings the magnetic flux from the interior to the atmosphere? (see Yuhong Fan's Living Reviews article)

- How does emerging flux transport the magnetic energy and helicity?

- How much flux is trapped below the surface during flux emergence, and what is the contribution of this trapped flux to the solar dynamo?

- What are the roles of emerging flux in the free energy accumulation and triggering of the transient events such as jets, flares, CMEs?

Science questions

- What are the physical properties of subsurface magnetic structures that rise and eventually emerge onto the surface?

- Does flux emergence occur as the rise of coherent bundles or as smaller elementary units? (Zwaan, 1978, 1985)?

- What is the difference between flare-productive sunspots and quiet sunspots?

- How do convective flows impact the morphology and physical character of emerging flux (e.g., Fan et al., 2003; Cheung et al., 2007a)?

Science questions

- How do the individual and statistical properties (e.g., Hagenaar, 2001; Hagenaar et al., 2003; Iida et al., 2012; Otsuji et al., 2011) of emerging flux relate to the solar activity cycle?

- What are the observational consequences of emerging magnetic flux (Bruzek, 1967; Zwaan, 1978), and what are the physical mechanisms responsible?

- Can we predict the appearance of new emerging flux regions?

- What are the physical ingredients necessary for a realistic model of emerging flux?

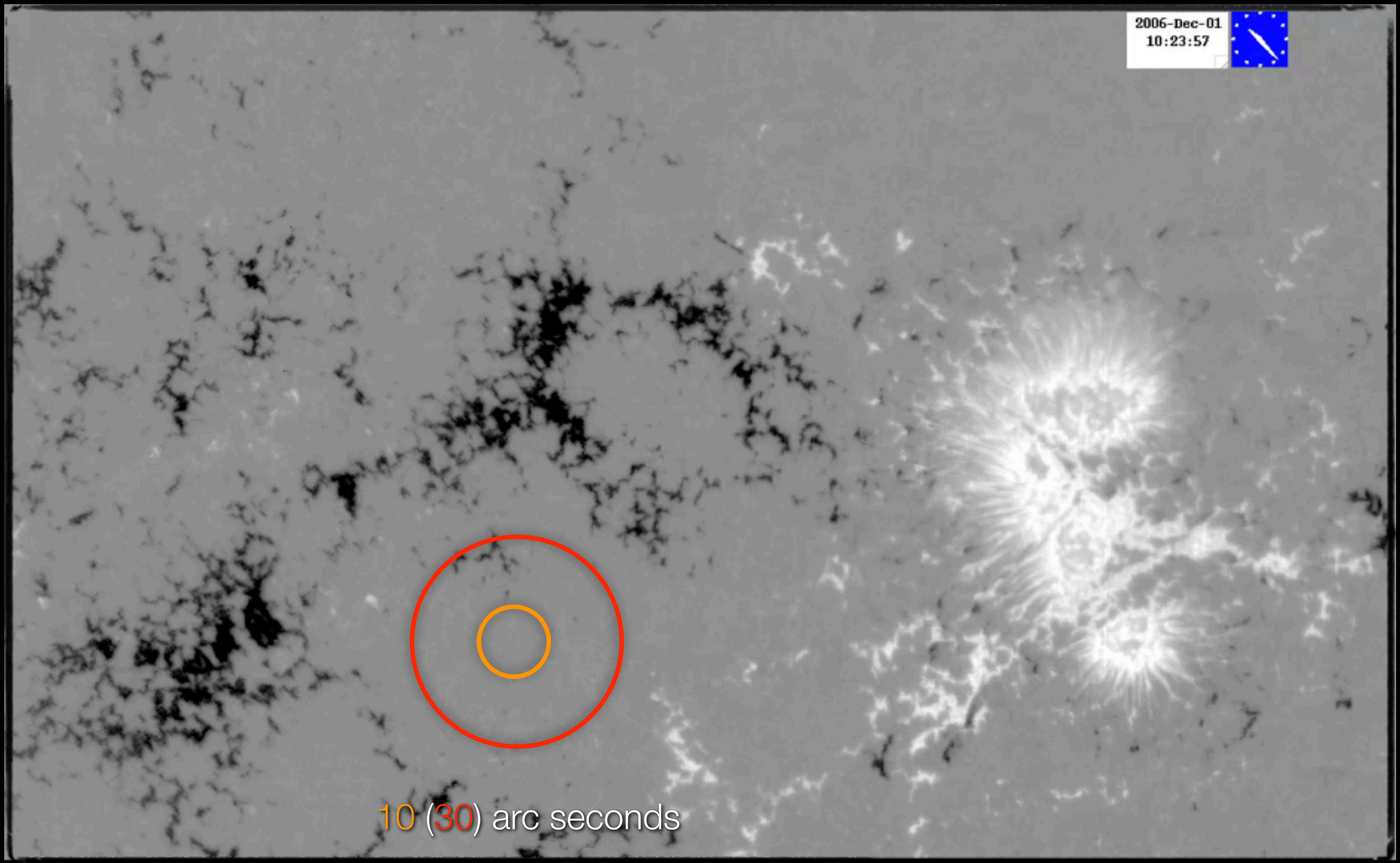

Hinode SOT observation trilobite (Credit: Title)

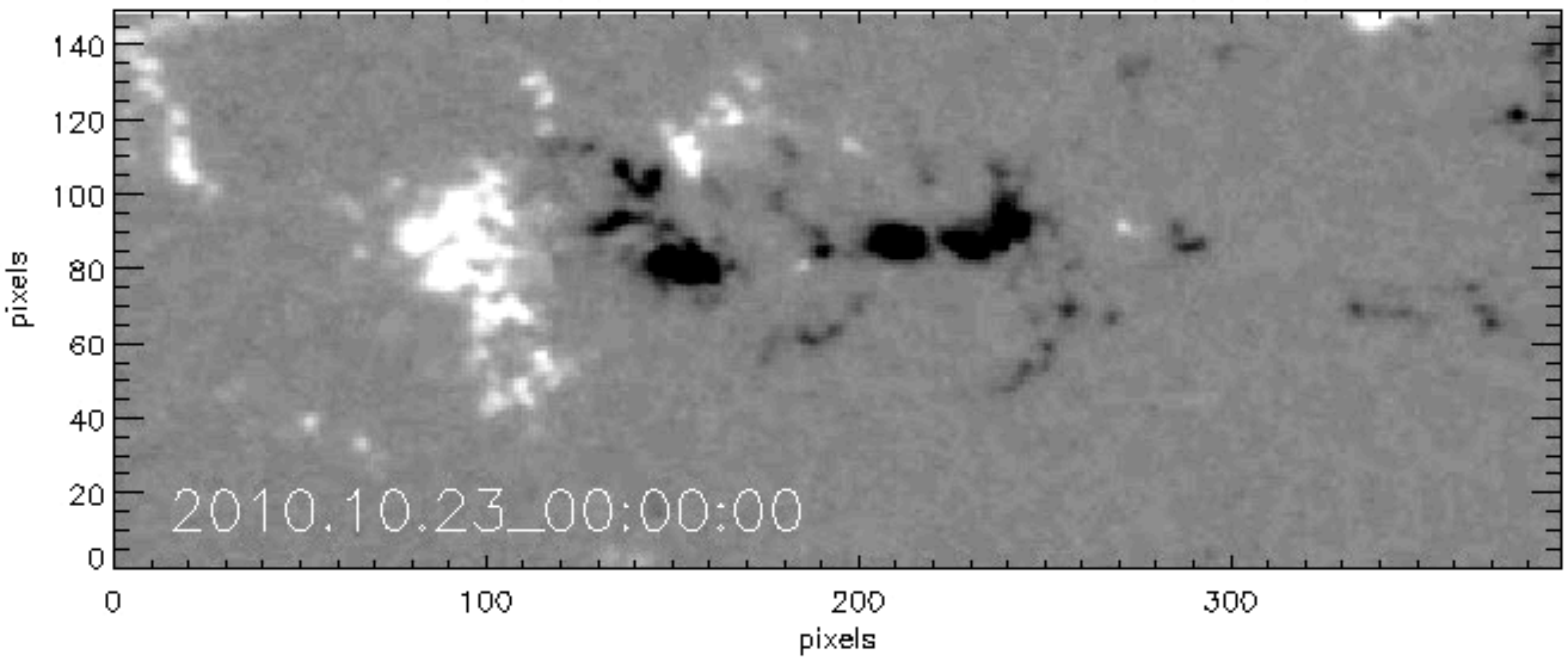

(Credit: Yang Liu, Stanford)

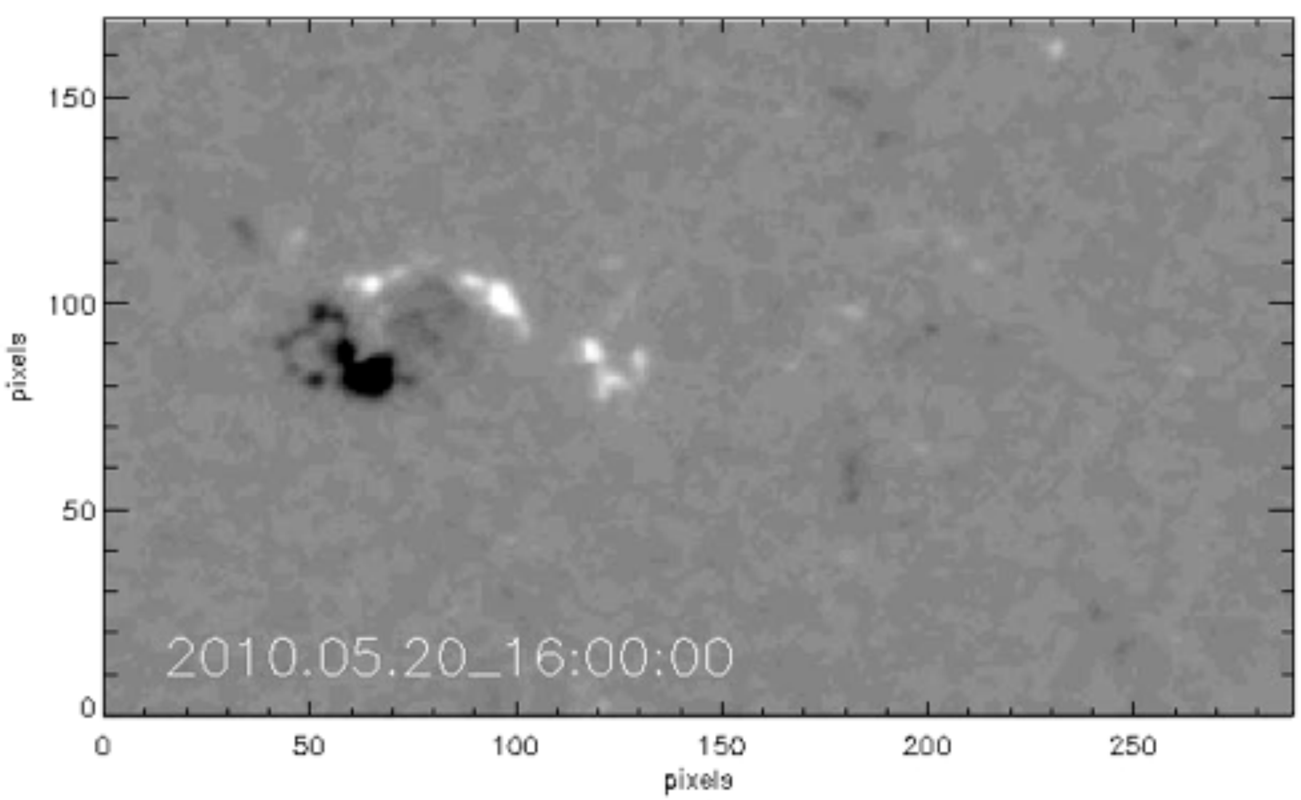

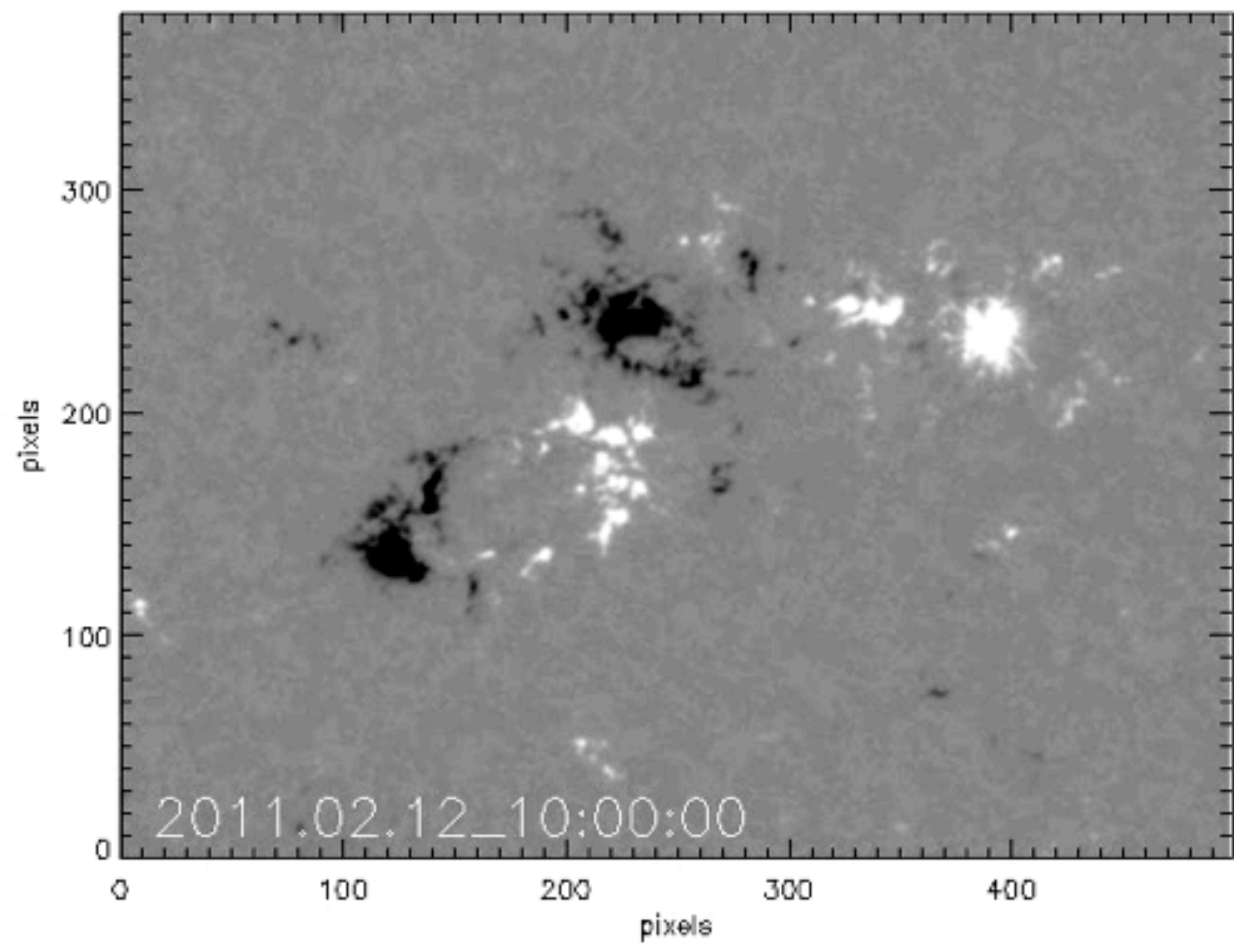

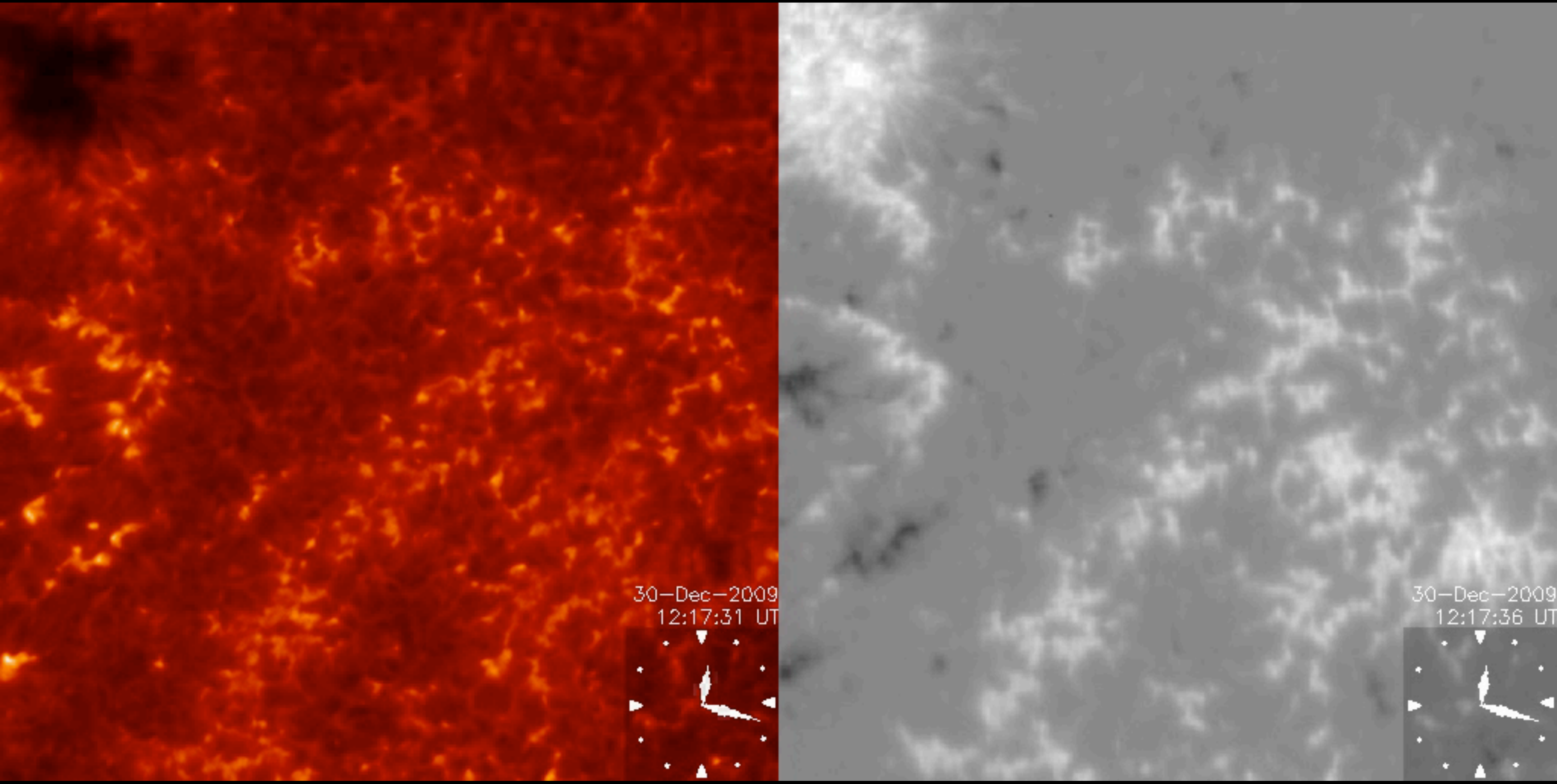

Hinode SOT observation of sunspot formation (Shimizu, Ichimoto & Suematsu 2012): A Ca II dark ring precedes appearance of the penumbra in G-band BFI images

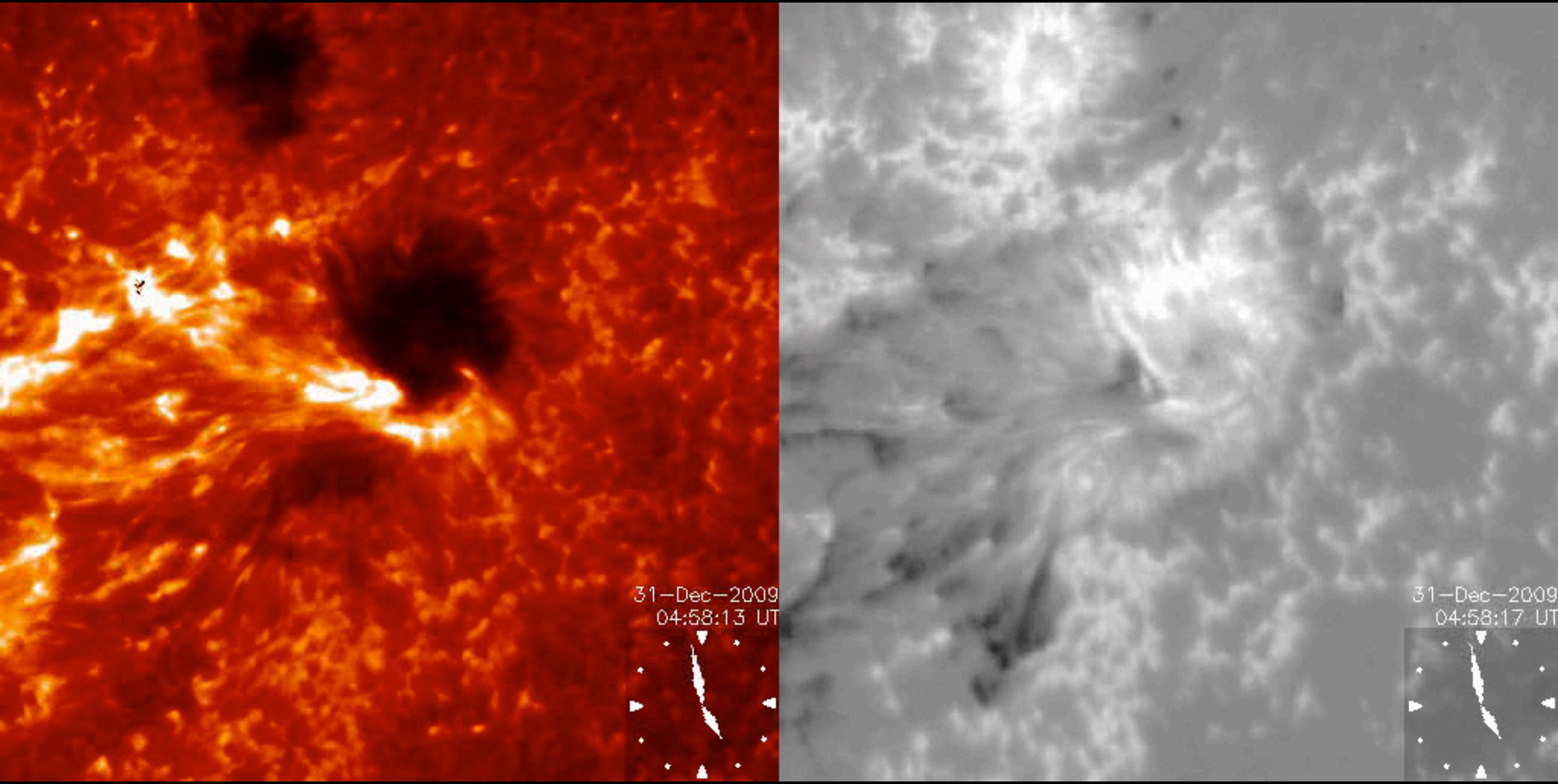

Hinode SOT observation of sunspot formation (Shimizu, Ichimoto & Suematsu 2012): A Ca II dark ring precedes appearance of the penumbra in G-band BFI images

A *fluid* view of MHD

Magnetohydrodynamics (MHD) captures the following physical principles:

- Mass conservation, $$\frac{D\varrho}{Dt} + \varrho\nabla\cdot\mathbf{v} = 0\,,$$
- Momentum conservation,
$$\varrho\frac{D\mathbf{v}}{Dt} = \nabla\cdot\underline{\sigma} + \varrho\mathbf{g},$$
$$\sigma_{ij} = -\underline{p}\delta_{ij} + M_{ij},$$
$$M_{ij} = -\frac{B^2}{8\pi}\delta_{ij} + \frac{B_iB_j}{4\pi}.$$
- Energy conservation, $$\varrho\frac{Ds}{Dt} = \frac{\underline{Q}}{T}\,,$$
- Faraday's law of induction. (next slide)

Faraday's Induction Equation

Faraday's induction equation is

$$\frac{\partial \mathbf{B}}{\partial t} = -c\nabla \times \underline{\mathbf{E}}\,, \tag{8}$$

where $\mathbf{E}$ is the electric field and c is the speed of light. In the regime of ideal MHD where the plasma is a perfect electrical conductor the electric field $\mathbf{E}'$ in the co-moving inertial frame of the plasma vanishes. Assuming the plasma velocity $\mathbf{v}$ has speed $|v| \ll c$, a Lorentz transformation to the 'lab' frame leads to

$$\mathbf{E} = -c^{-1}\mathbf{v} \times \mathbf{B}\,. \tag{9}$$

This yields the familiar Eulerian form of the ideal MHD induction equation

$$\frac{\partial \mathbf{B}}{\partial t} = \nabla \times (\mathbf{v} \times \mathbf{B})\,. \tag{10}$$

In Lagrangian form, this equation becomes

$$\frac{D\mathbf{B}}{Dt} = -\mathbf{B}(\nabla \cdot \mathbf{v}) + (\mathbf{B} \cdot \nabla)\mathbf{v}\,. \tag{11}$$

Fluid expansion / compression

Stretching flow along magnetic field lines intensifies B

Faraday's Induction Equation

Faraday's induction equation is

$$\frac{\partial \mathbf{B}}{\partial t} = -c\nabla \times \mathbf{E}, \tag{8}$$

where $\mathbf{E}$ is the electric field and c is the speed of light. In the regime of ideal MHD where the plasma is a perfect electrical conductor the electric field $\mathbf{E}'$ in the co-moving inertial frame of the plasma vanishes. Assuming the plasma velocity $\mathbf{v}$ has speed $|v| \ll c$, a Lorentz transformation to the 'lab' frame leads to

$$\mathbf{E} = -c^{-1}\mathbf{v} \times \mathbf{B}\,. \tag{9}$$

This yields the familiar Eulerian form of the ideal MHD induction equation

$$\frac{\partial \mathbf{B}}{\partial t} = \nabla \times (\mathbf{v} \times \mathbf{B})\,. \tag{10}$$

In Lagrangian form, this equation becomes

$$\frac{D\mathbf{B}}{Dt} = -\mathbf{B}(\nabla \cdot \mathbf{v}) + (\mathbf{B} \cdot \nabla)\mathbf{v}\,. \tag{11}$$

Fluid expansion / compression

Stretching flow along magnetic field lines intensifies B

Constitutive Relations

Equation of State $p = p(\varrho,\varepsilon),\ s = s(\varrho,\varepsilon),\ T = T(\varrho,\varepsilon)$

Ohm's Law $c\boldsymbol{E} = -\boldsymbol{v}\times\boldsymbol{B} + \eta\boldsymbol{\nabla}\times\boldsymbol{B}$

Diffusion coefficients $\boldsymbol{\sigma},\ Q = \boldsymbol{\nabla}\cdot(\kappa\boldsymbol{\nabla}\mathbf{T}),\ \eta$

Radiative properties $Q = -\boldsymbol{\nabla}\cdot(\boldsymbol{F}_{\mathrm{rad}})$

Constitutive relations are statements about the material properties of the medium (in this case, plasma). The choice of different constitutive relations spawns a diversity of MHD models.

A Diversity of MHD Models

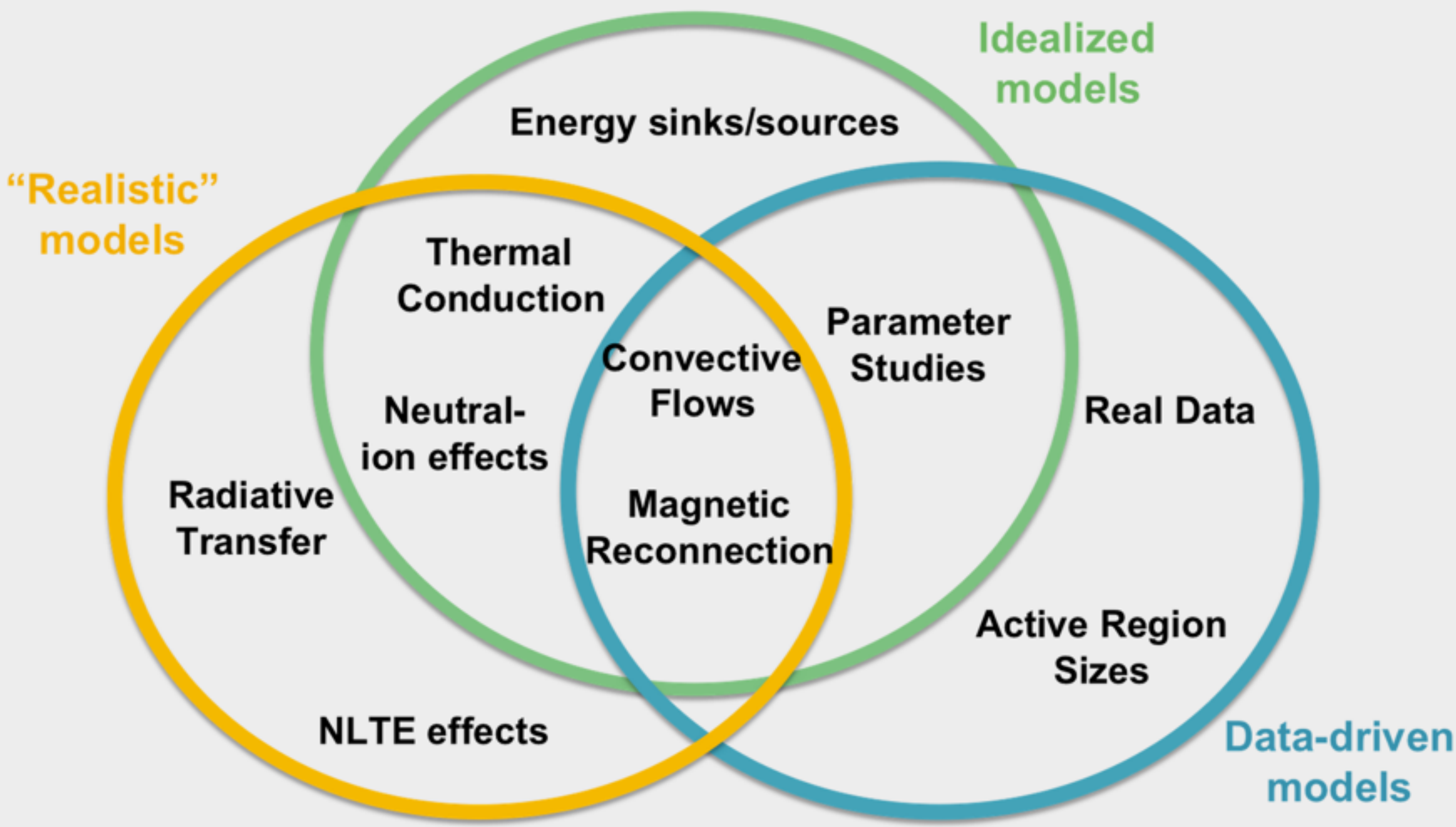

Figure 5: Models of magnetic flux emergence can be roughly divided into three categories, though there are large areas of overlap between them. So-called 'realistic' models attempt to include all the known important physical ingredients, while idealize models generally focus on studying a more limited set of effects. For case studies of certain observed emerging flux studies, data-driven models are used.

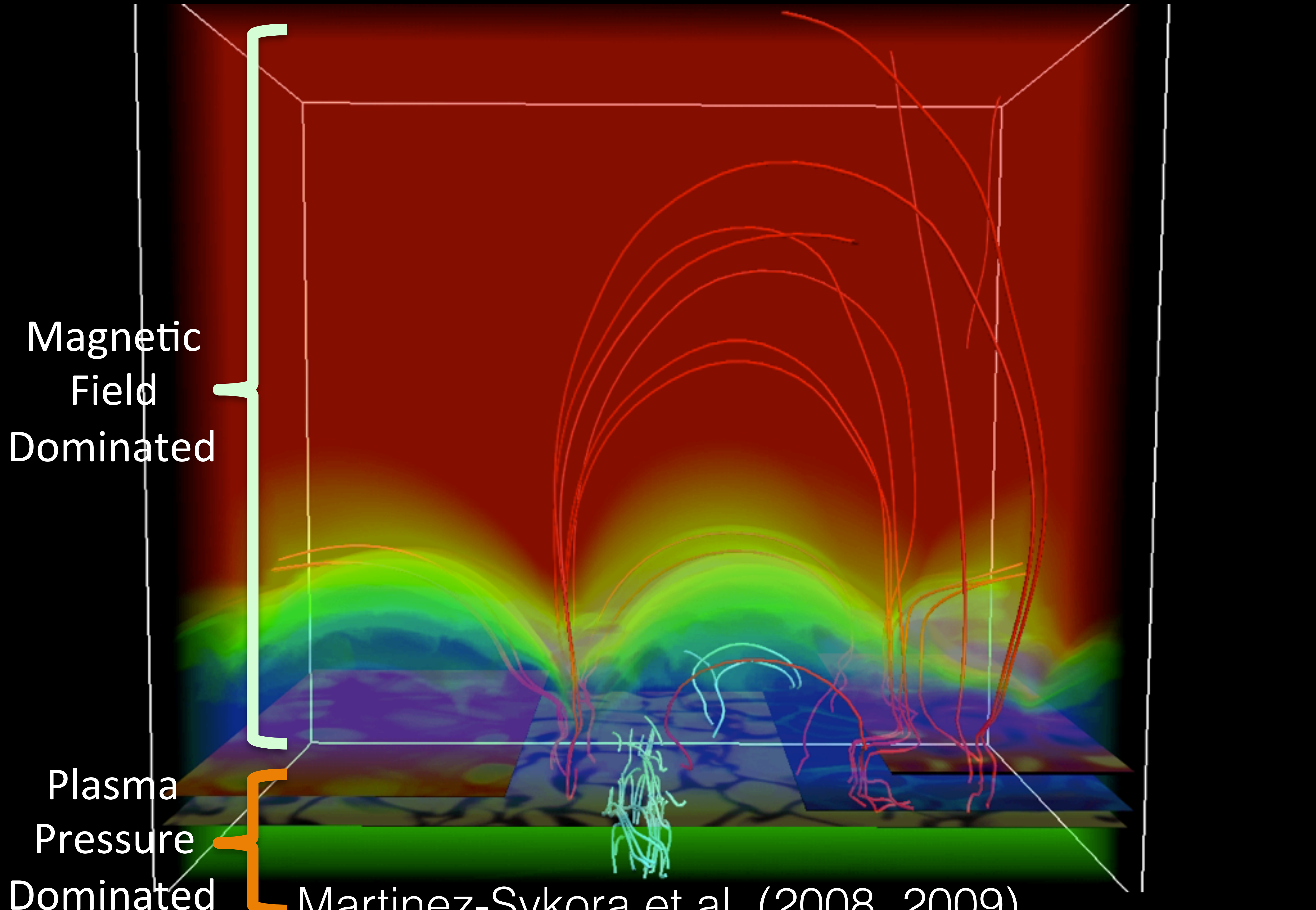
Magnetic
Field
Dominated
Plasma
Pressure
Dominated
Martinez-Sykora et al. (2008, 2009)


Buoyancy

Magnetic Buoyancy (Parker 1955)

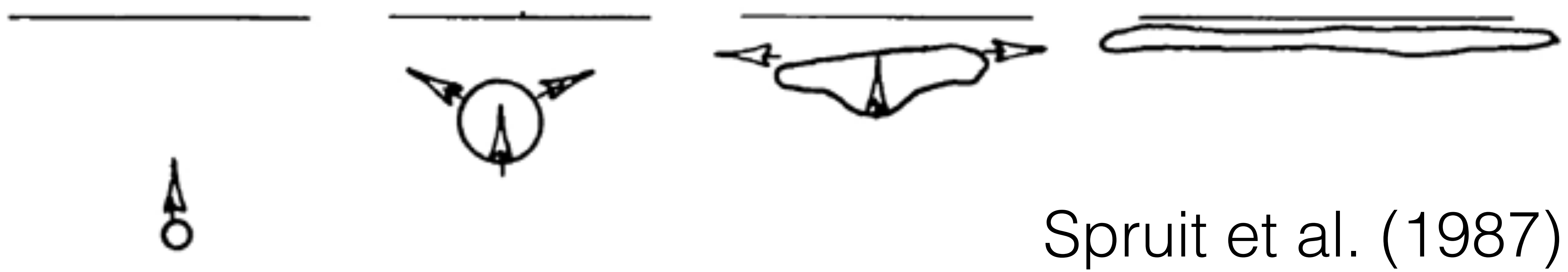

Spruit et al. (1987)

Consider a blob of plasma threaded by ***B***, which exhibits magnetic pressure $B^2/8\pi$. When the blob is in pressure balance with its surroundings,

$$p_{in} + B^2/8\pi = p_{ext.}$$

If the plasma blob has the same temperature or specific entropy as the surrounding (i.e. $T_{in} = T_{ext}$, or $s_{in} = s_{ext}$), then it will have a **density deficit**, and hence will rise like an air bubble.

Surface

$0.0000001\ g/cm^3$

Gravitational Stratification

- The solar convection zone is highly stratified.

Depth = 200,000 km

$0.1\ g/cm^3$

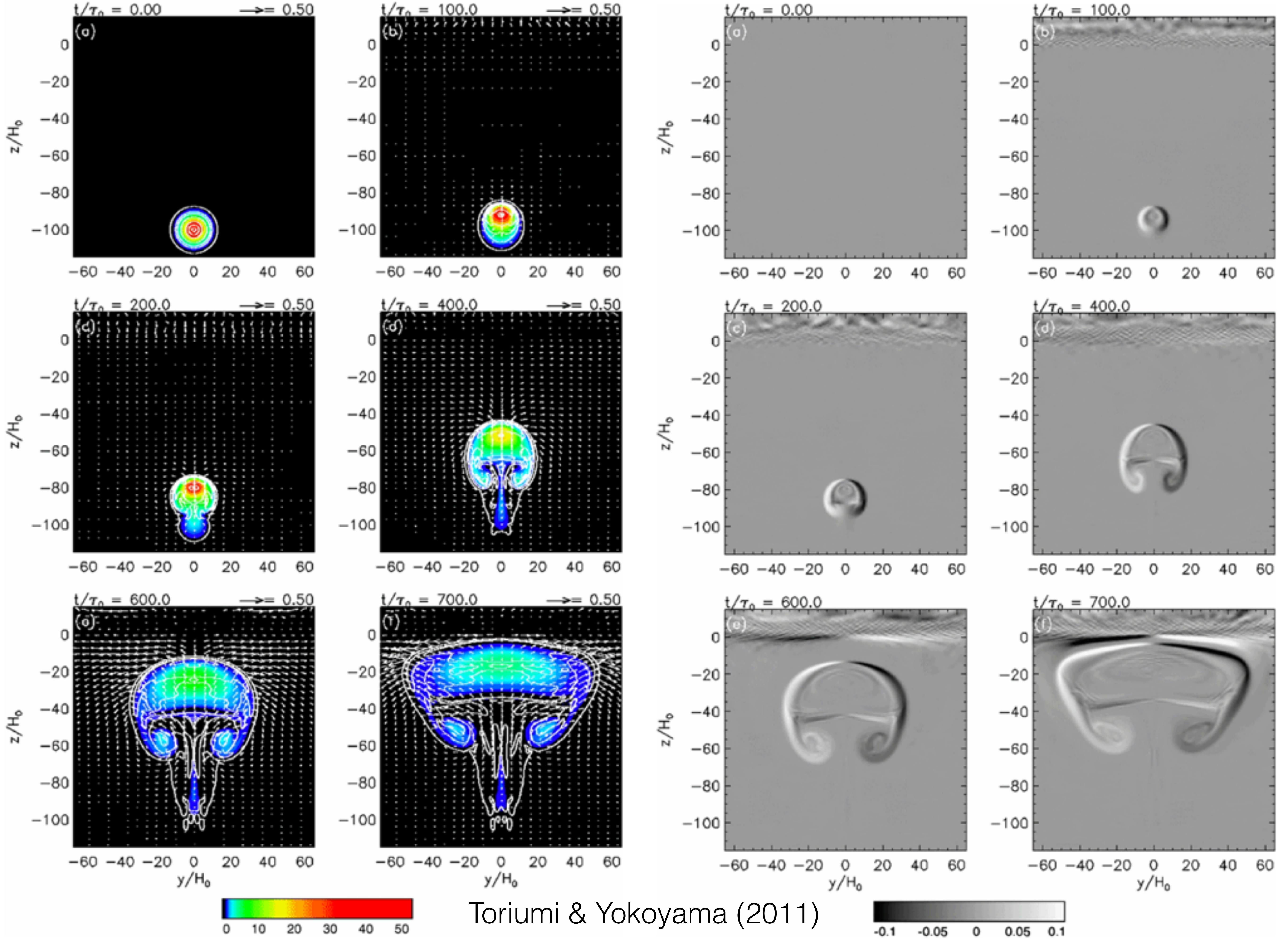

Toriumi & Yokoyama (2011)

Scaling Relation Between B and ϱ

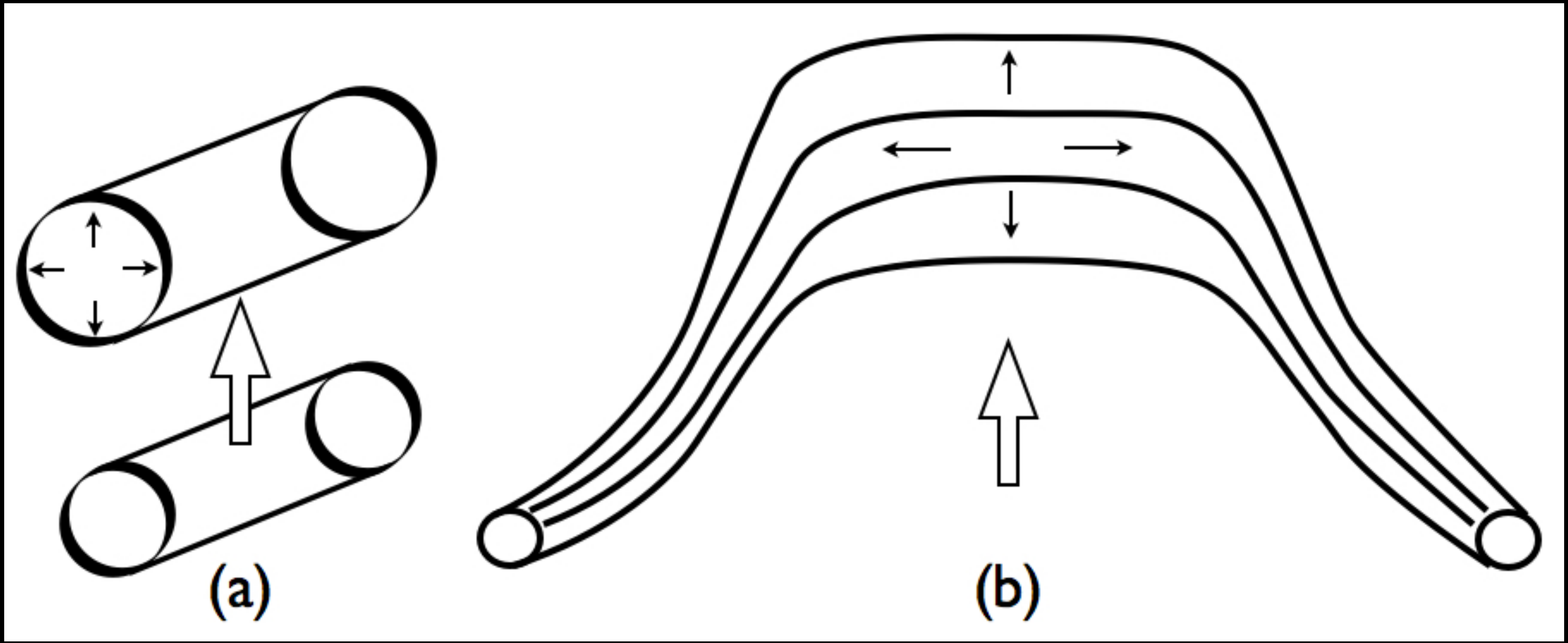

(a) Horizontal tube expanding as it rises

$B \propto \varrho$

(b) Crest of tube expanding predominantly in the horizontal directions

$B \propto \varrho^{1/2}$

Flux Emergence Workshop 2011 @ SSL

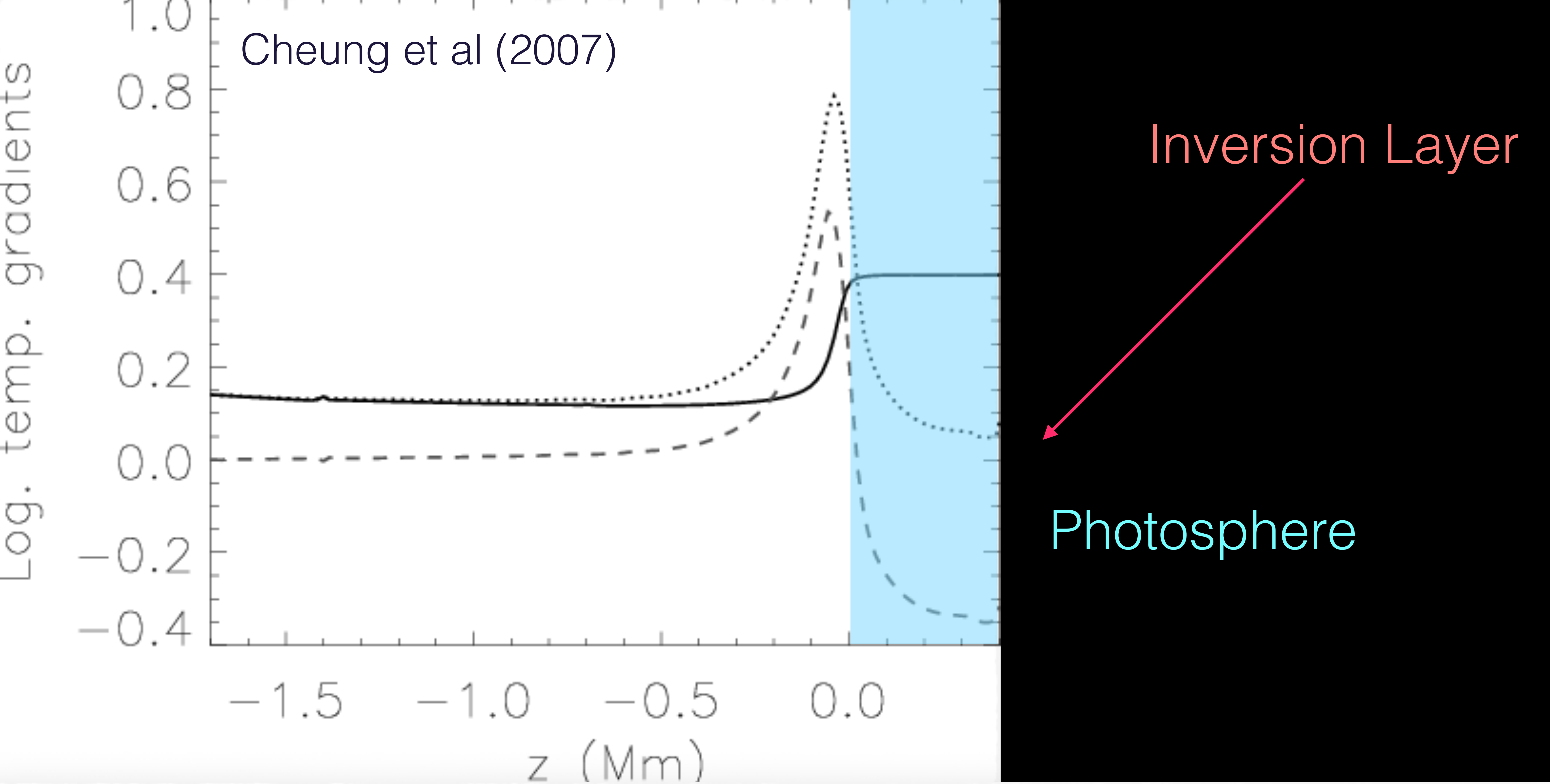

The classifications of the convective (in)stability of a stratification can be phrased in terms of logarithmic temperature gradients. The Schwarzschild criterion states that a stratification is convectively unstable if $\nabla > \nabla_{\rm ad}$, where

$$\nabla_{\rm ad} = \left.\frac{d\ln T}{d\ln p}\right|_s , \tag{25}$$

$$\nabla = \frac{d\ln T}{d\ln p} . \tag{26}$$

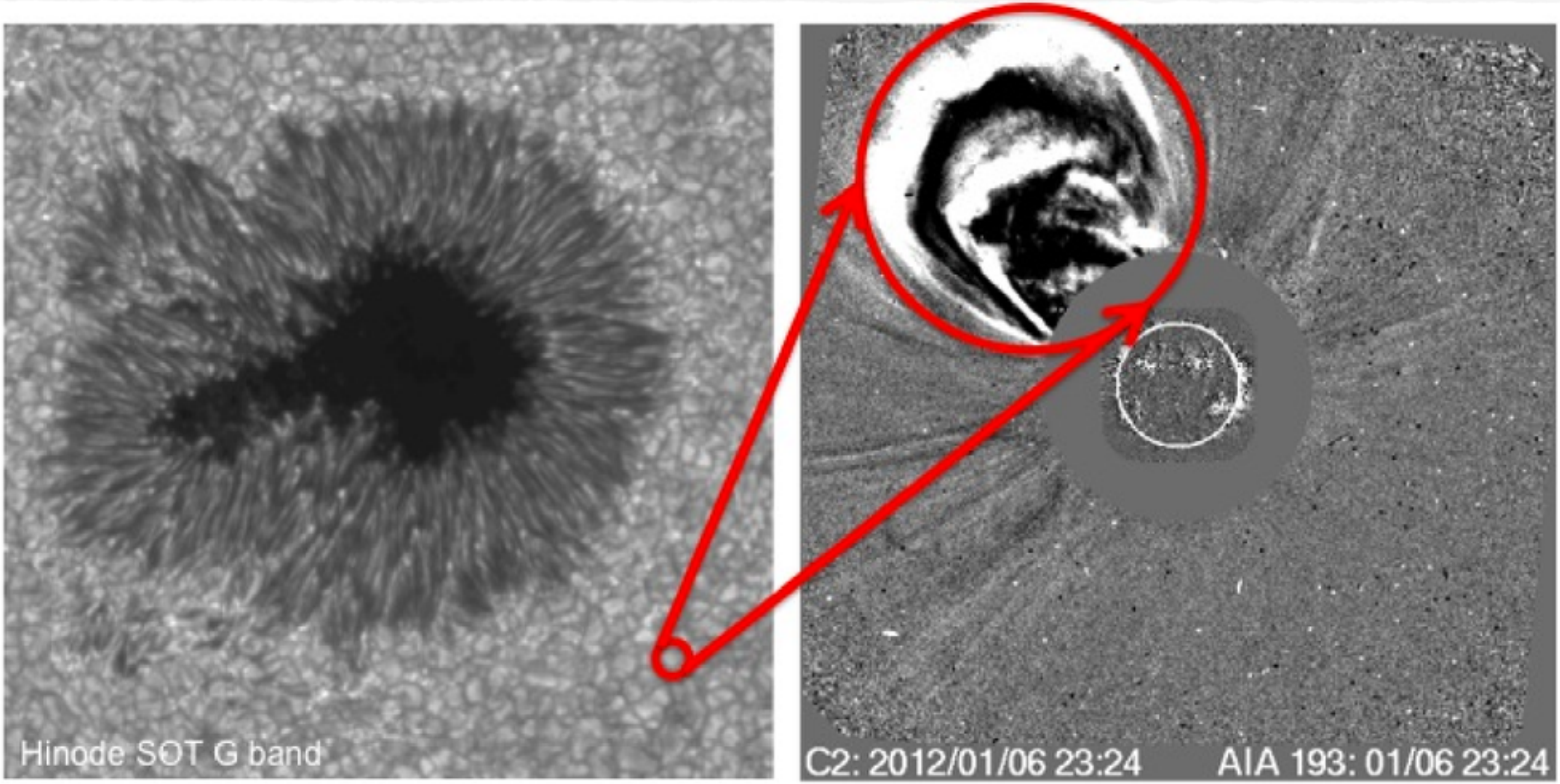

Figure 13: The solar atmosphere is strongly stratified: the mass contained in a single granule (left, Hinode SOT image of a sunspot surrounded by granulation) is comparable to the mass content of the largest CMEs (right, composite of running difference images from the SOHO/LASCO C2 and SDO/AIA instruments. Both quantities are of order 10^{16} g. (Credit for right image: NASA CDAW Data Center.)

Buoyancy Instabilities

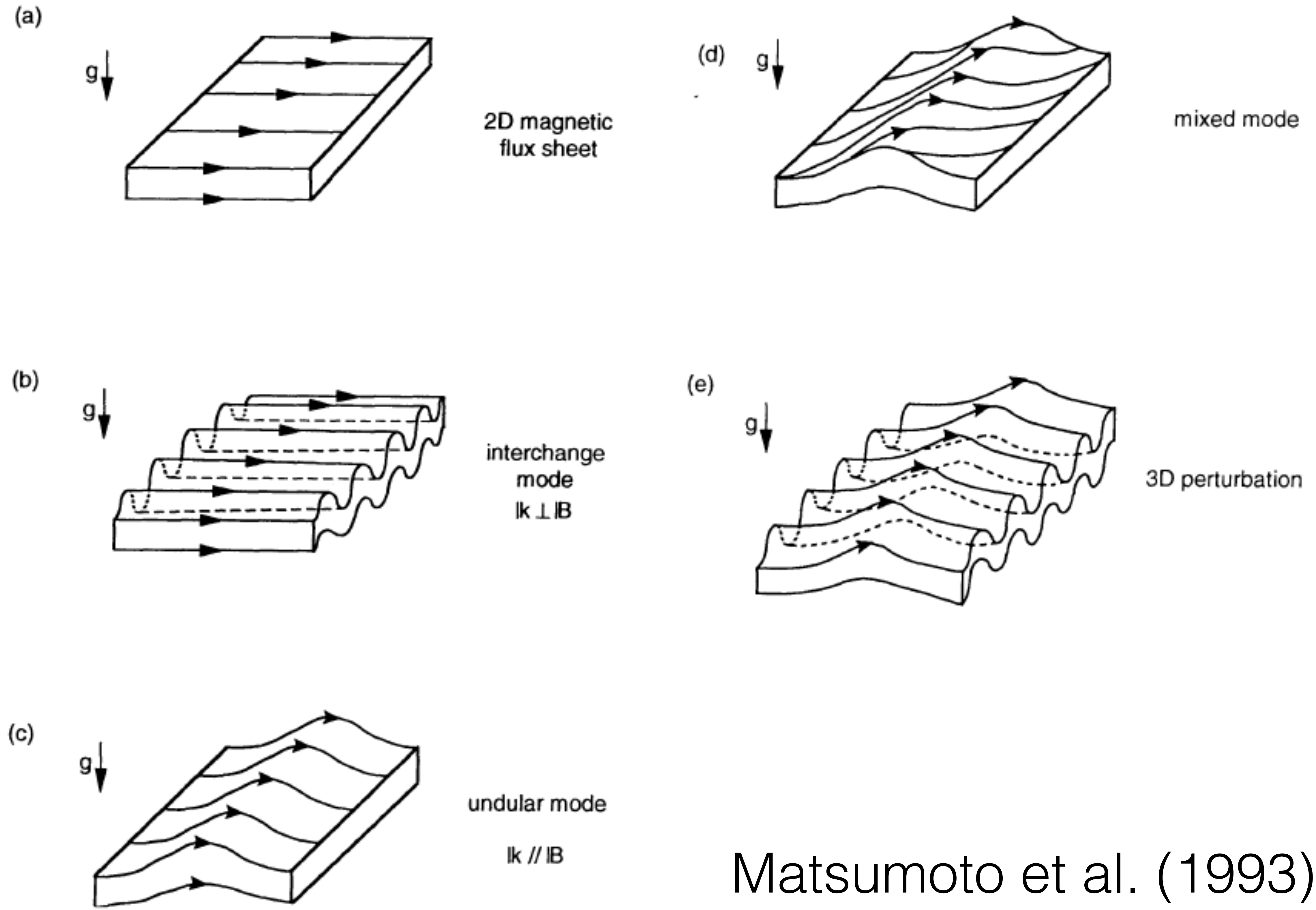

Matsumoto et al. (1993)

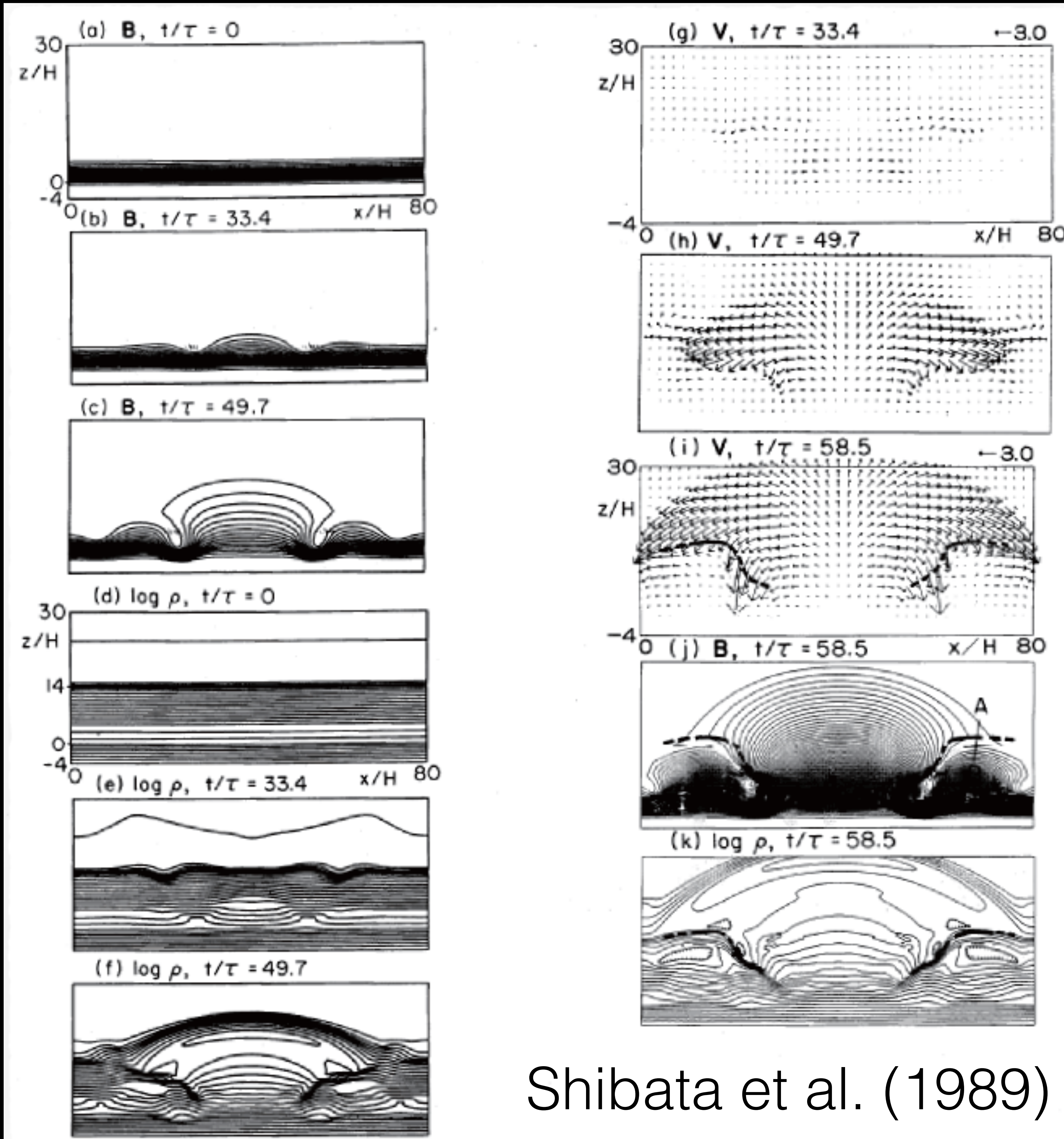

Shibata et al. (1989)

Non-linear development of the undular (Parker) mode

Magara (2001)

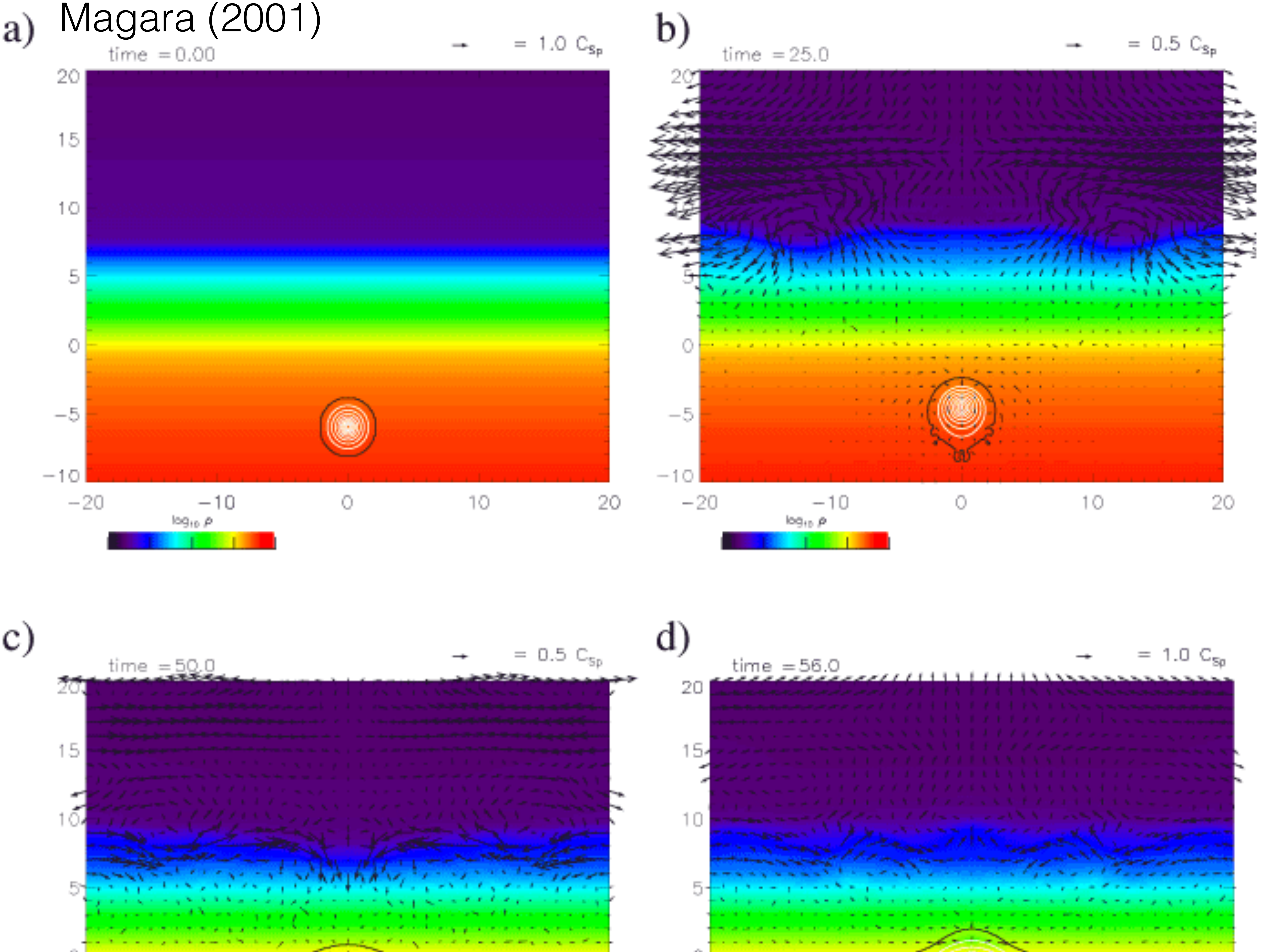
a)
time = 0.00
= 1.0 C_{Sp}
log₁₀ ρ
b)
time = 25.0
= 0.5 C_{Sp}
log₁₀ ρ
c)
time = 50.0
= 0.5 C_{Sp}
d)
time = 56.0
= 1.0 C_{Sp}

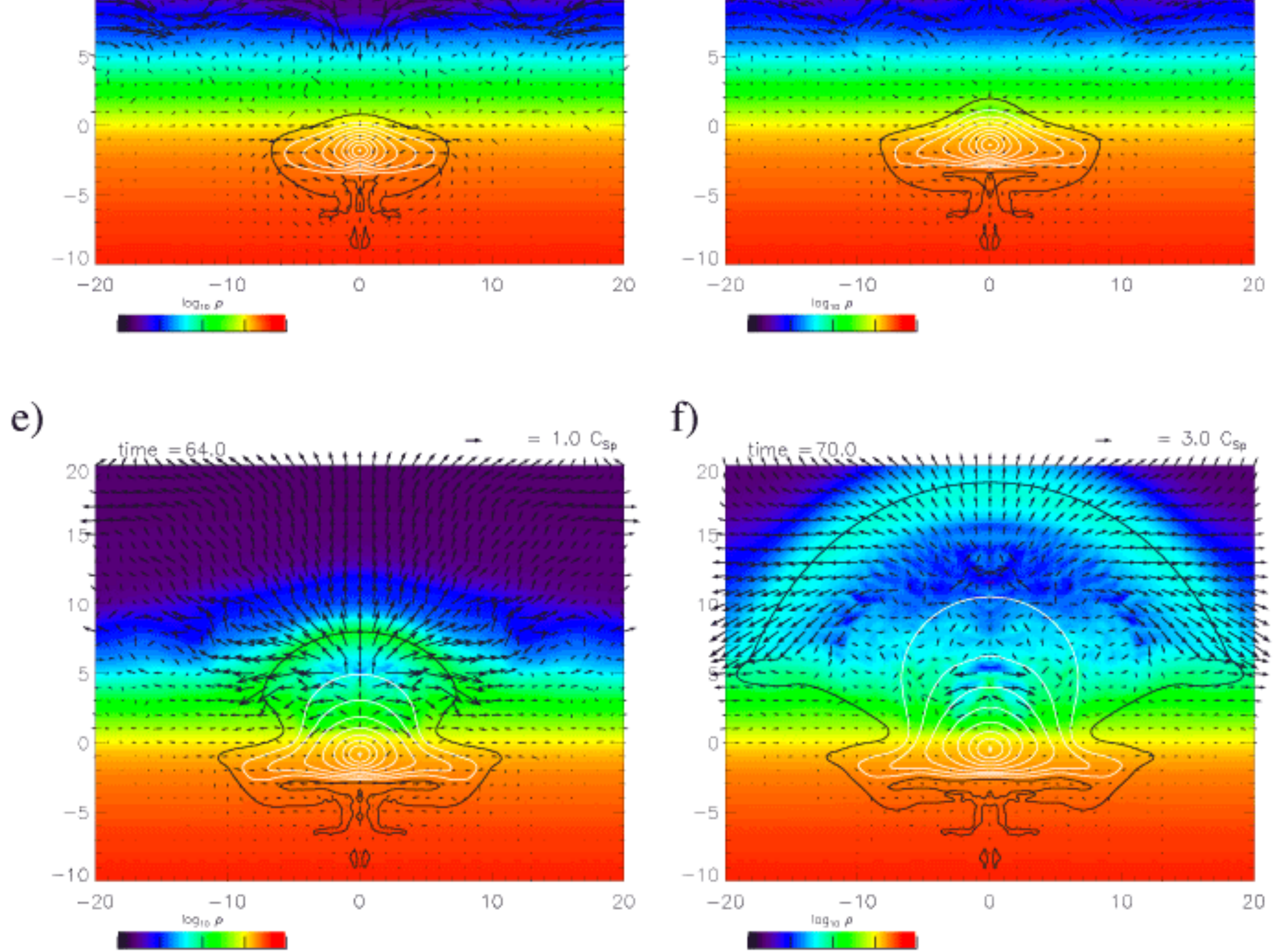

e)
time = 64.0
= 1.0 C_Sp
f)
time = 70.0
= 3.0 C_Sp
20
15
10
5
0
−5
−10
−20
−10
0
10
20
log10 ρ

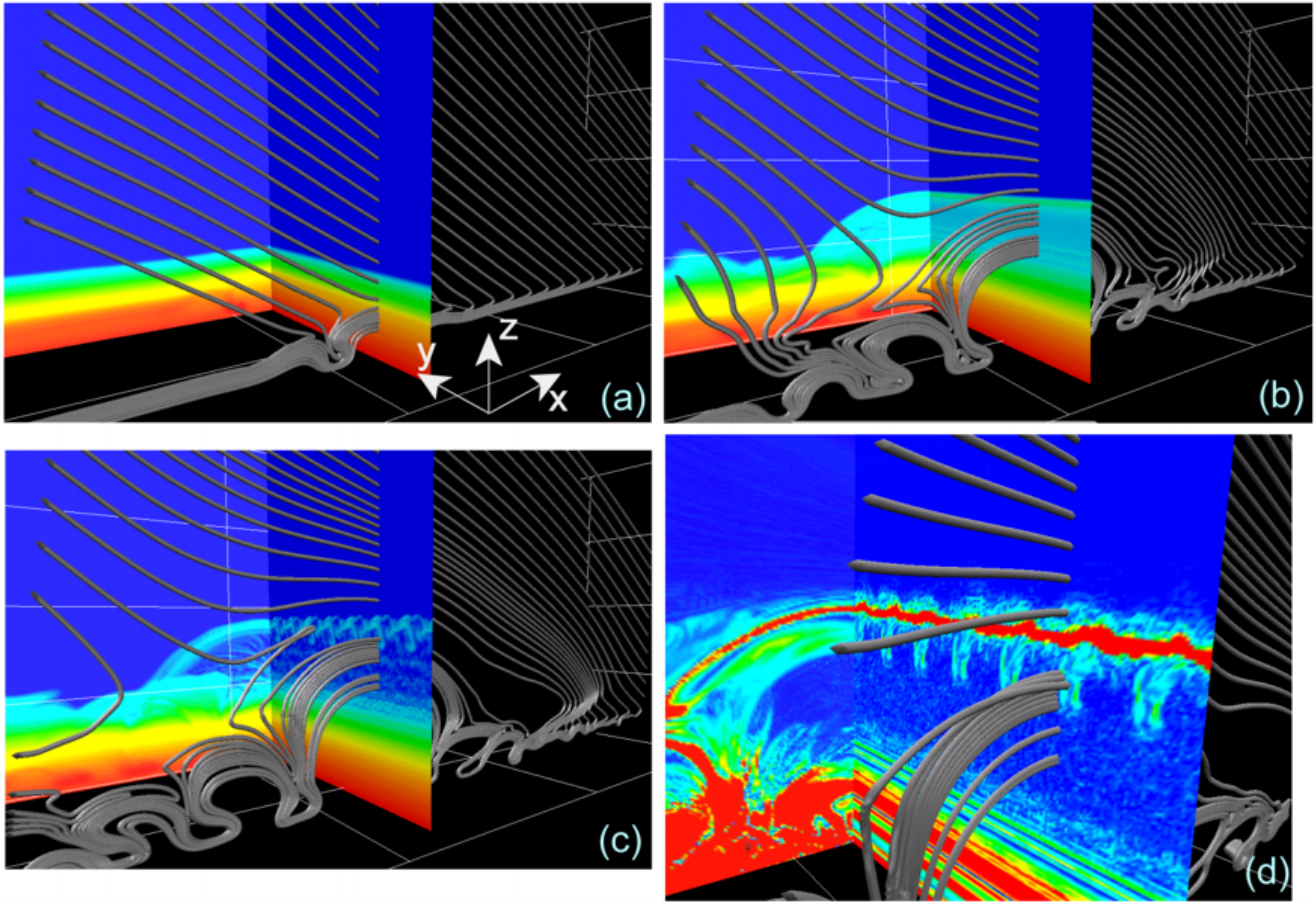

Isobe et al (2007)


Convection

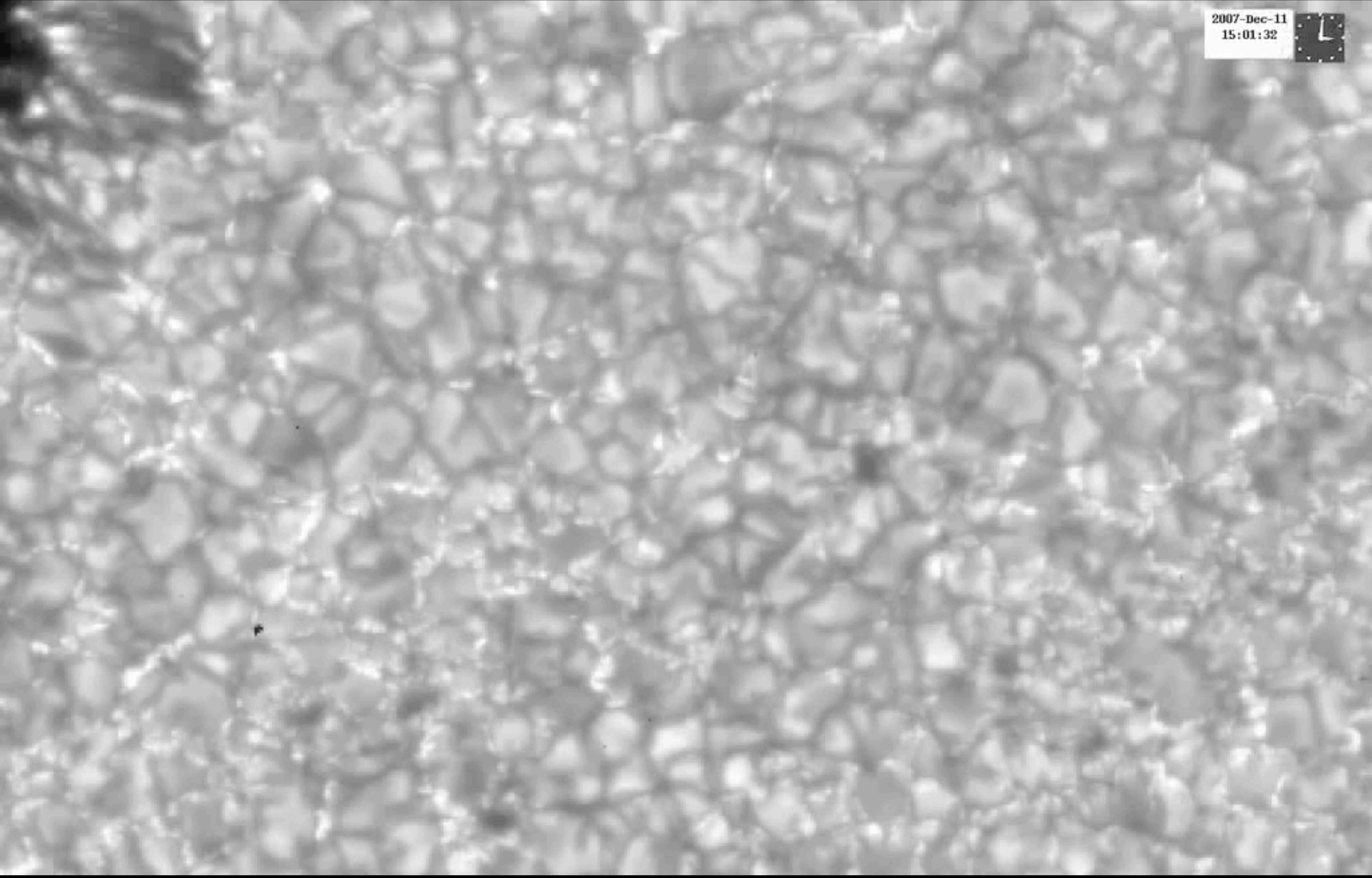

Hinode/SOT observation of an emerging flux region

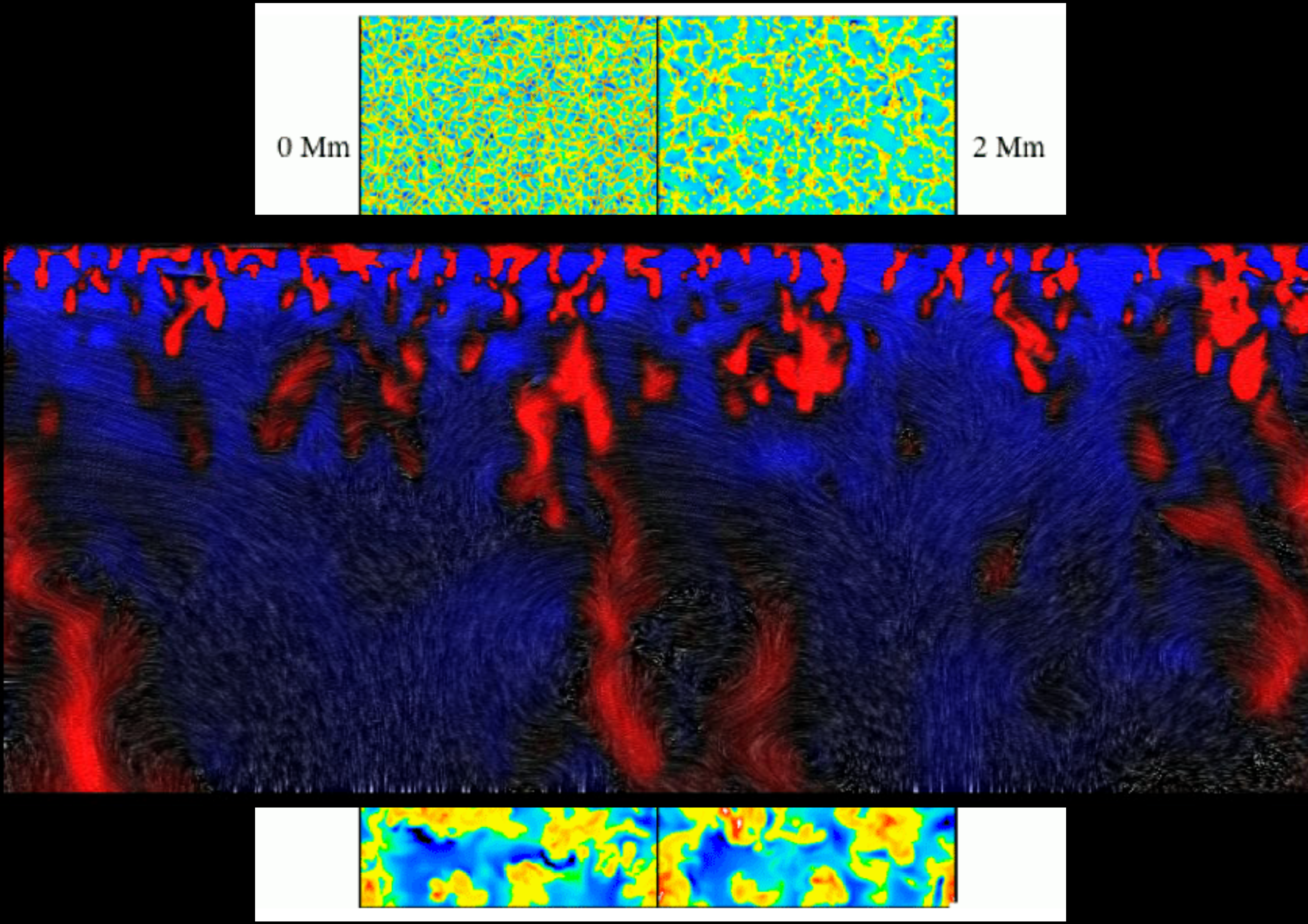

Vertical velocity structure at various depths (Stein et al 2011)

Surface Intensification of Emerging Magnetic Field

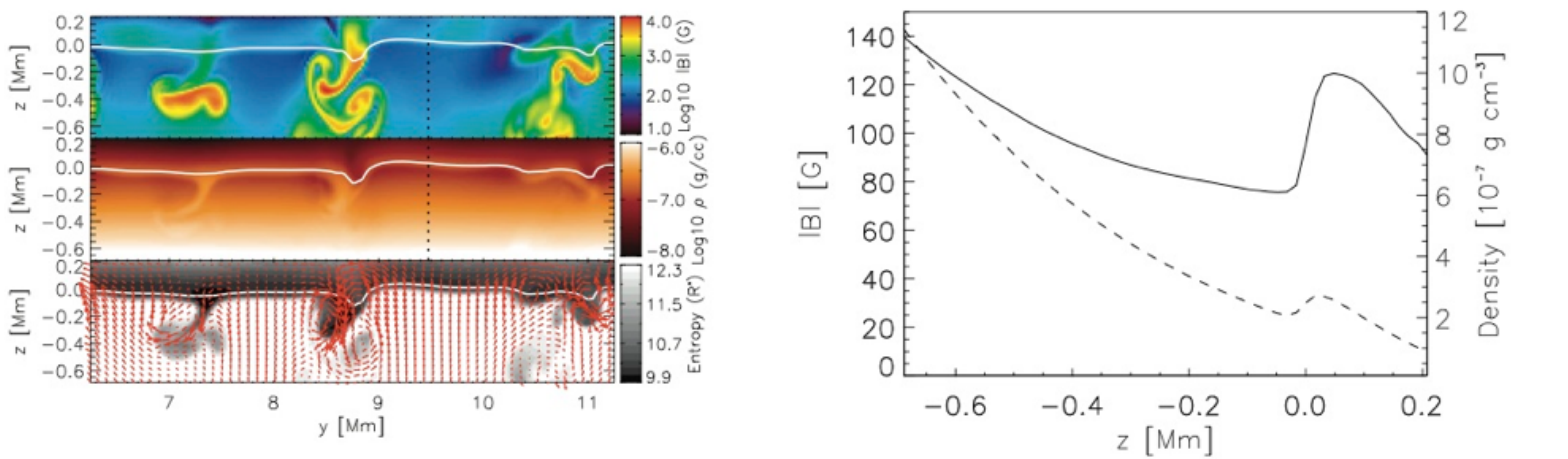

From Cheung et al. 2008: When a magnetic parcel reaches the photosphere and radiatively cools, its density and magnetic field strength enhances to give an inversion layer. The relative enhancement for |B| is greater than for mass density due to field stretching.

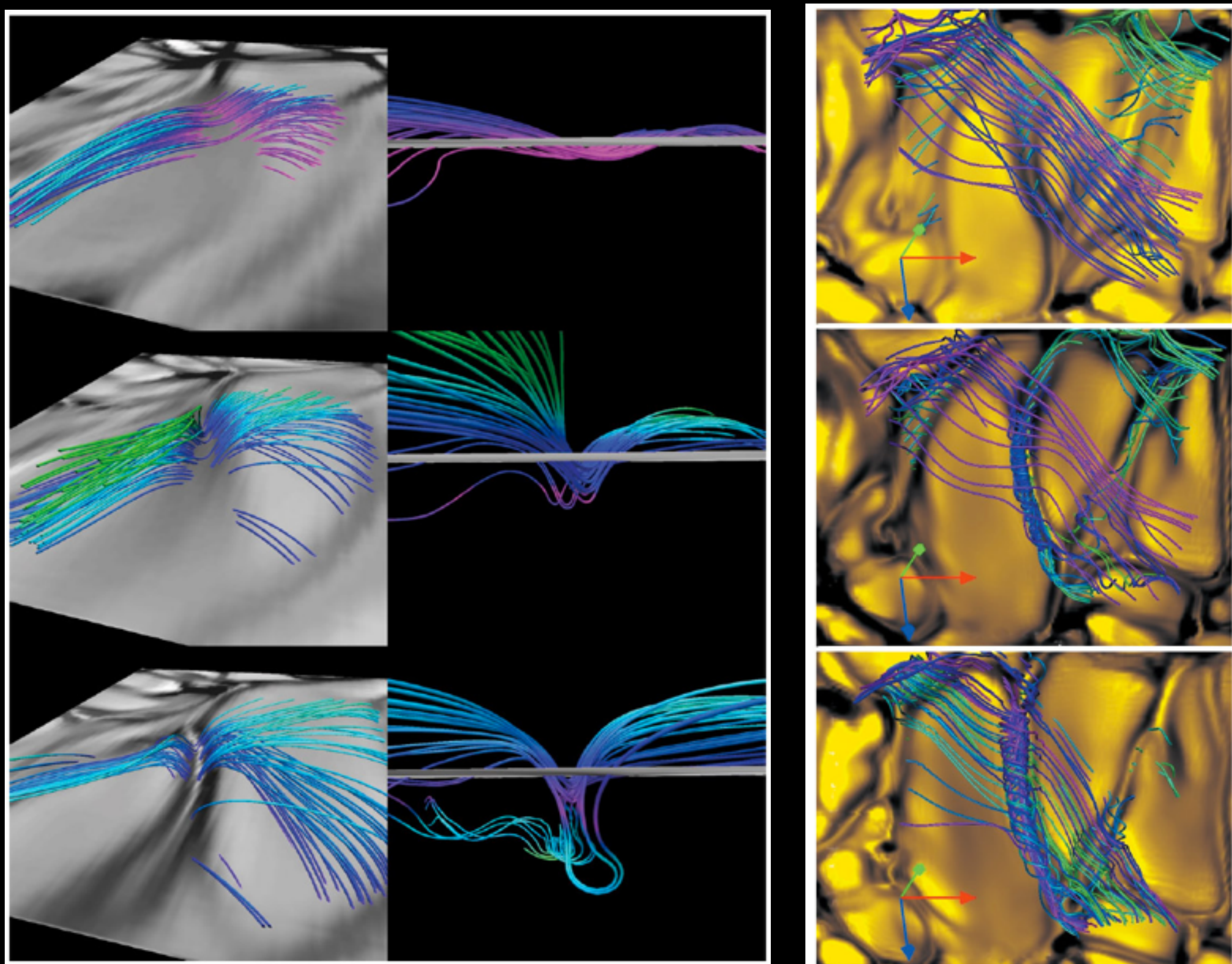

Tortosa-Andreu & Moreno-Insertis (2009)

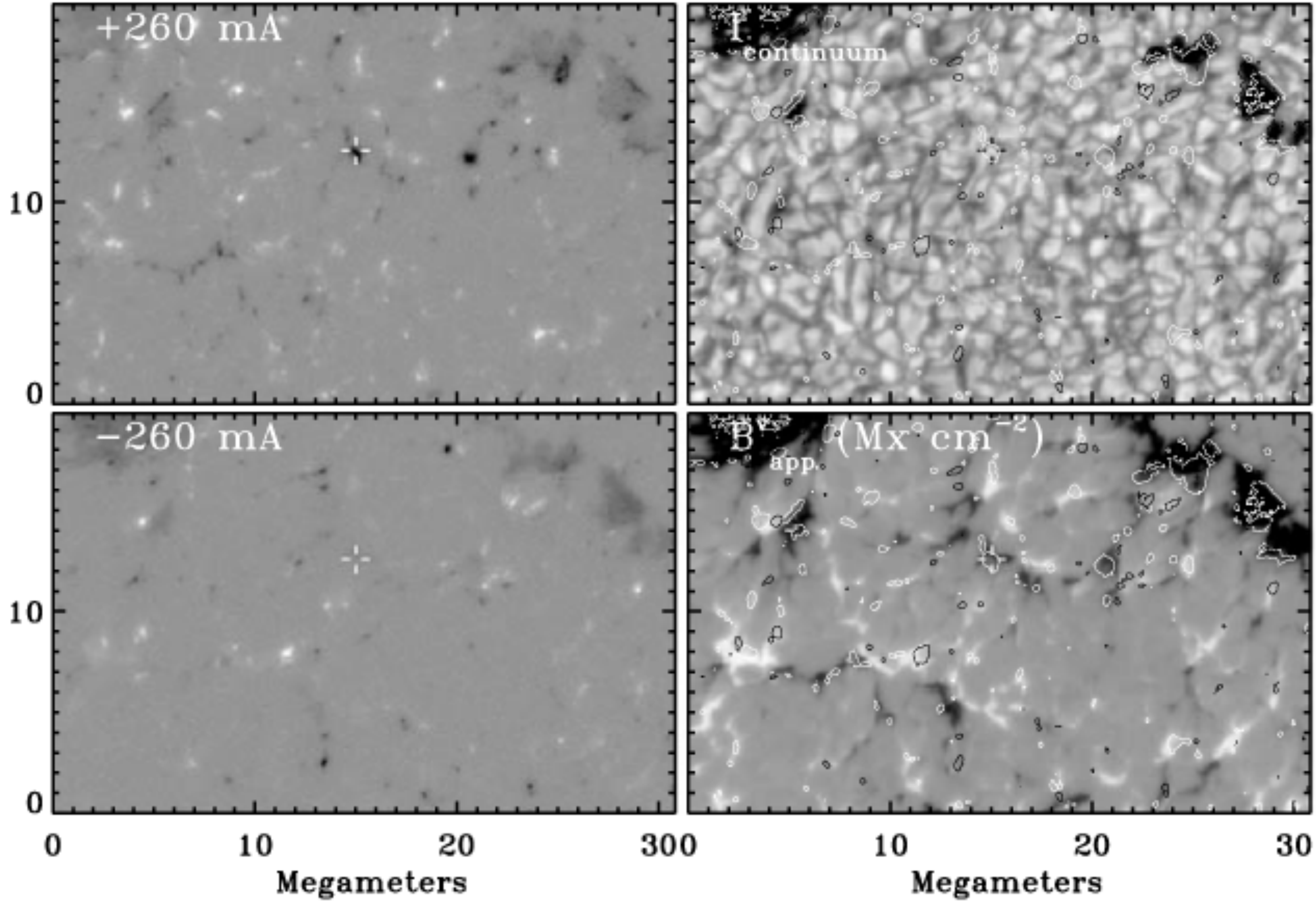

Lites (2009): Hinode/SP scan of an emerging flux region

Radiative MHD simulation of AR formation (Cheung et al. 2010)

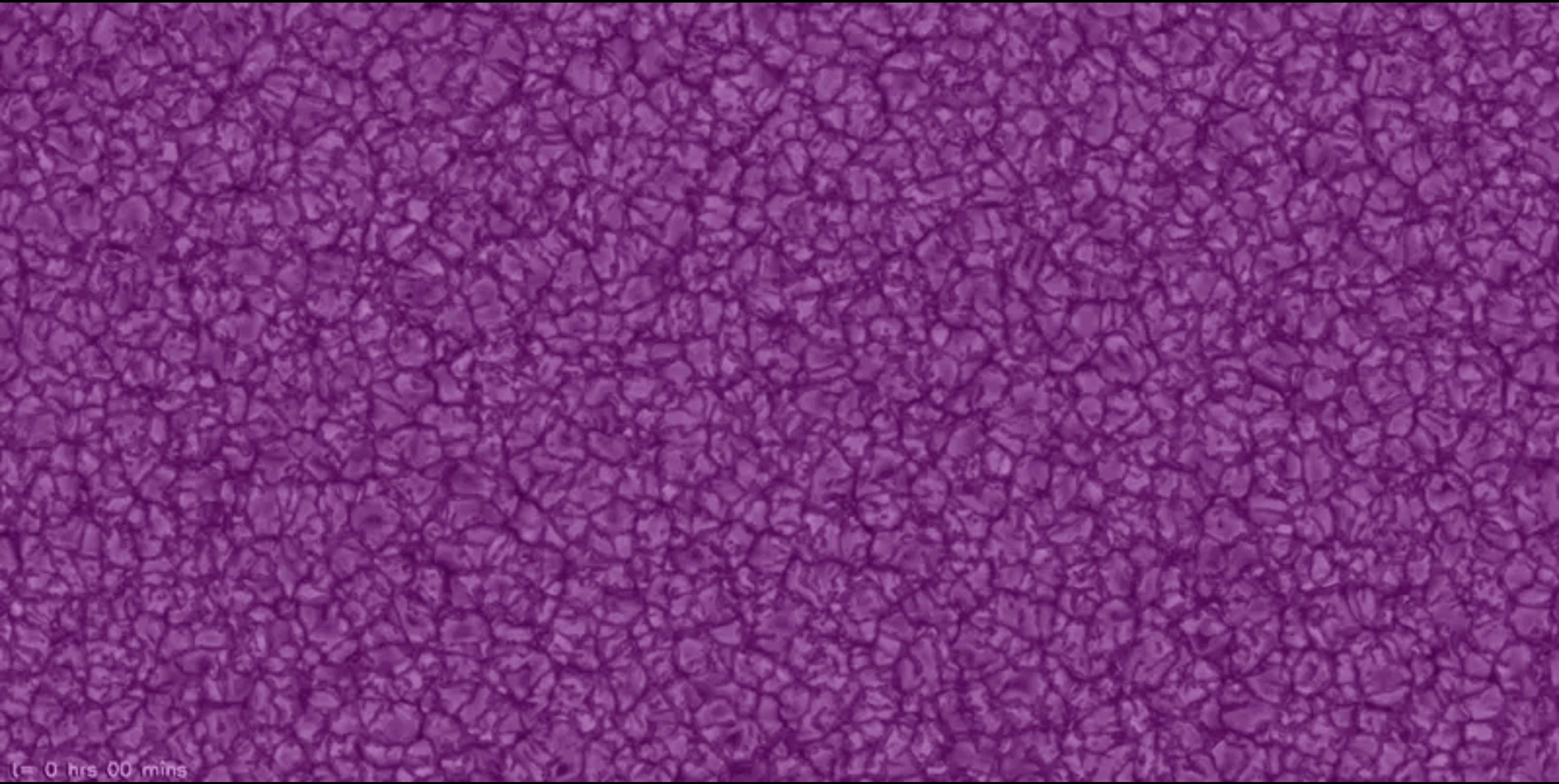

Red (negative magnetic flux) Green (horizontal magnetic field) Blue (positive magnetic flux)

Purple background (brightness intensity of convective flows)

Mass discharge

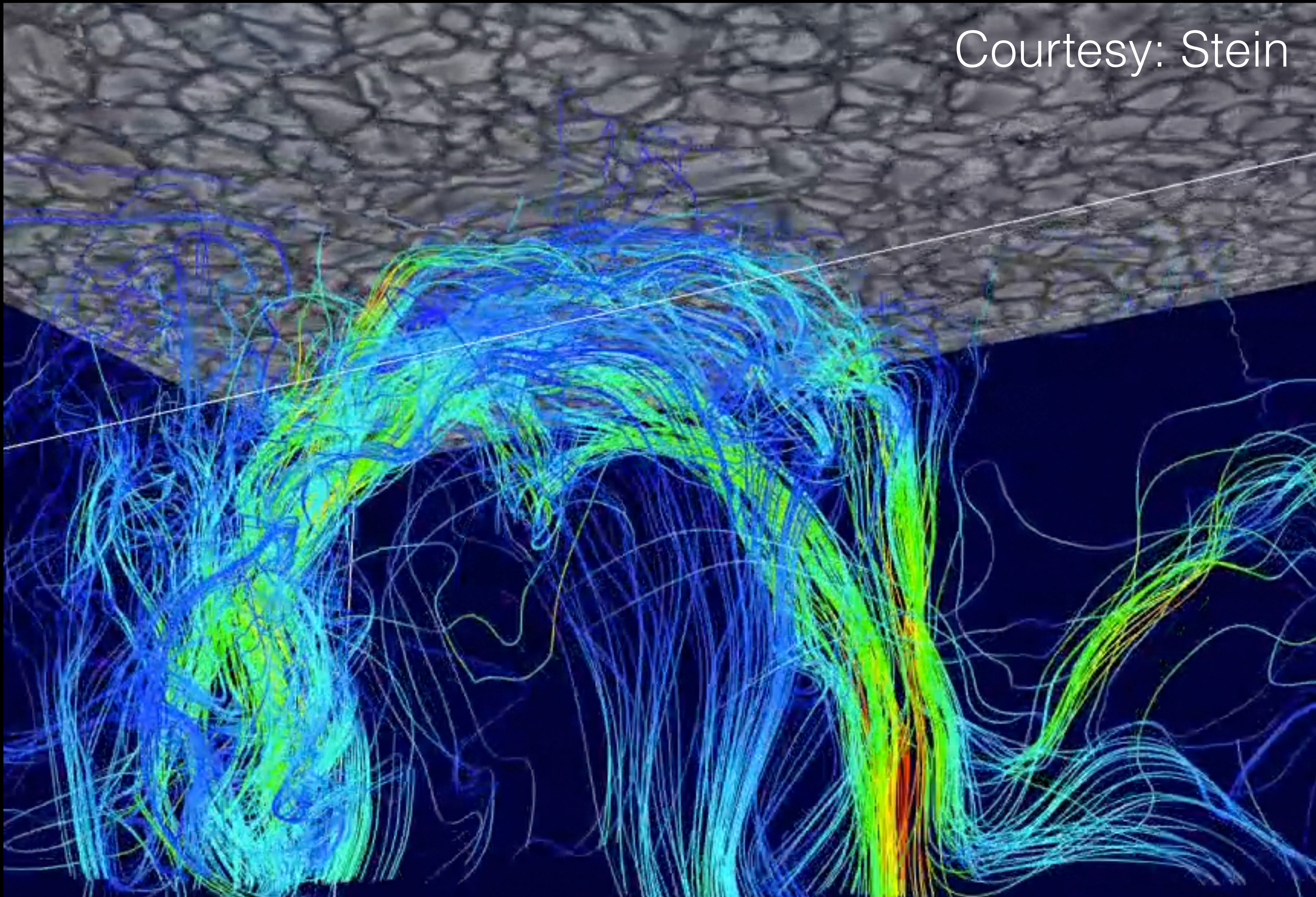

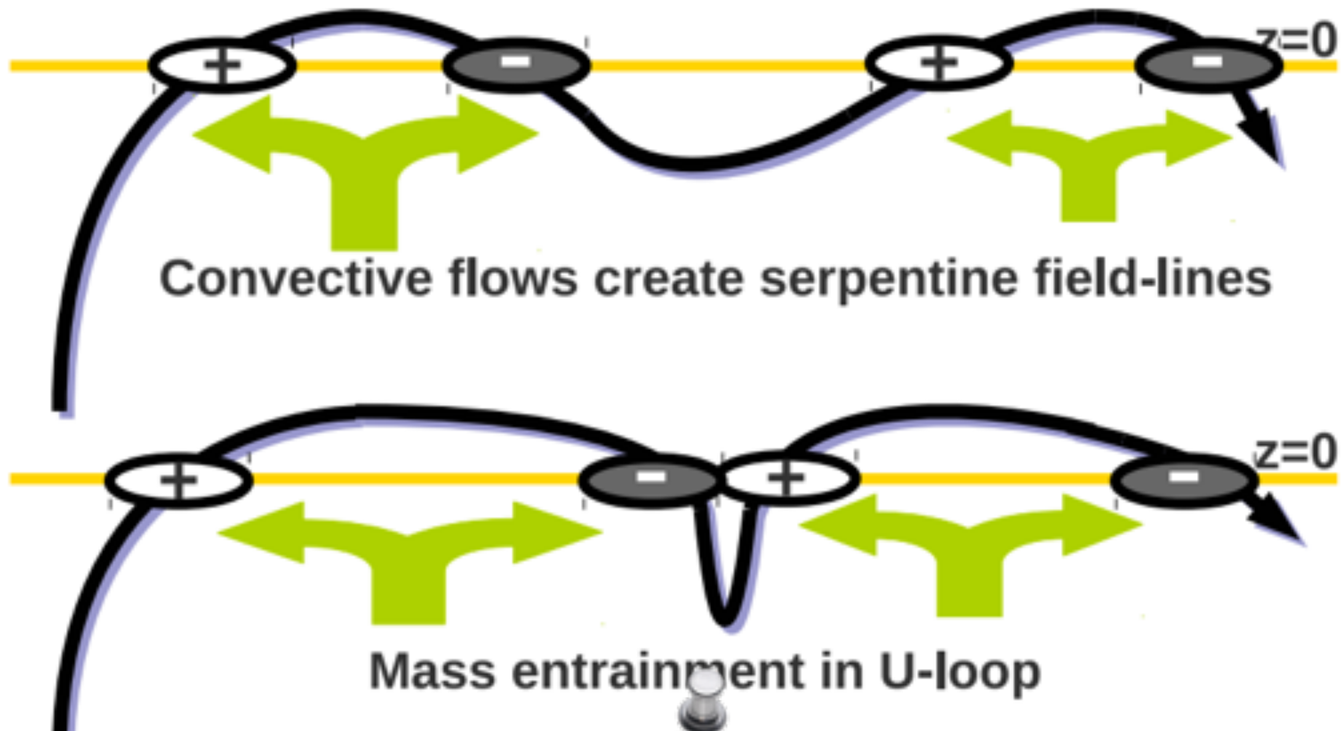

$$\frac{\partial \overline{\mathbf{B}}}{\partial t} = \nabla \times (\overline{\mathbf{v}} \times \overline{\mathbf{B}}) + \nabla \times E \,, \tag{34}$$

where $E = \overline{\mathbf{v}' \times \mathbf{B}'}$ is the (azimuthally-averaged) mean-field electromotive force resulting from correlations between the magnetic field and velocity field fluctuations (Krause and Rädler, 1980; Rädler, 1980). The time rate of change of magnetic flux crossing the circular surface $\mathcal{C}$ is then

$$\dot{\Phi}_{\mathcal{C}} = \int_{\mathcal{C}} \frac{\partial \overline{\mathbf{B}}}{\partial t} \cdot \mathbf{d}S = \oint_{\partial \mathcal{C}} \left(\overline{\mathbf{v}} \times \overline{\mathbf{B}} + E \right) \cdot \mathbf{d}l \,, \tag{35}$$

$$= \dot{\Phi}_{\mathrm{m}} + \dot{\Phi}_{\mathrm{f}} \,, \tag{36}$$

where

$$\dot{\Phi}_{\mathrm{m}} = 2\pi R [\overline{\mathbf{v}} \times \overline{\mathbf{B}}]_\theta = 2\pi R (\overline{v}_z \overline{B}_r - \overline{B}_z \overline{v}_r) \,, \tag{37}$$

$$\dot{\Phi}_{\mathrm{f}} = 2\pi R \mathcal{E}_\theta = 2\pi R \overline{v'_z B'_r - B'_z v'_r} \,. \tag{38}$$

Figure 37: Schematic drawing illustrating the effect of granular flows on magnetic polarities from a serpentine field line. Image reproduced with permission from Cheung *et al.* (2010), copyright by AAS.

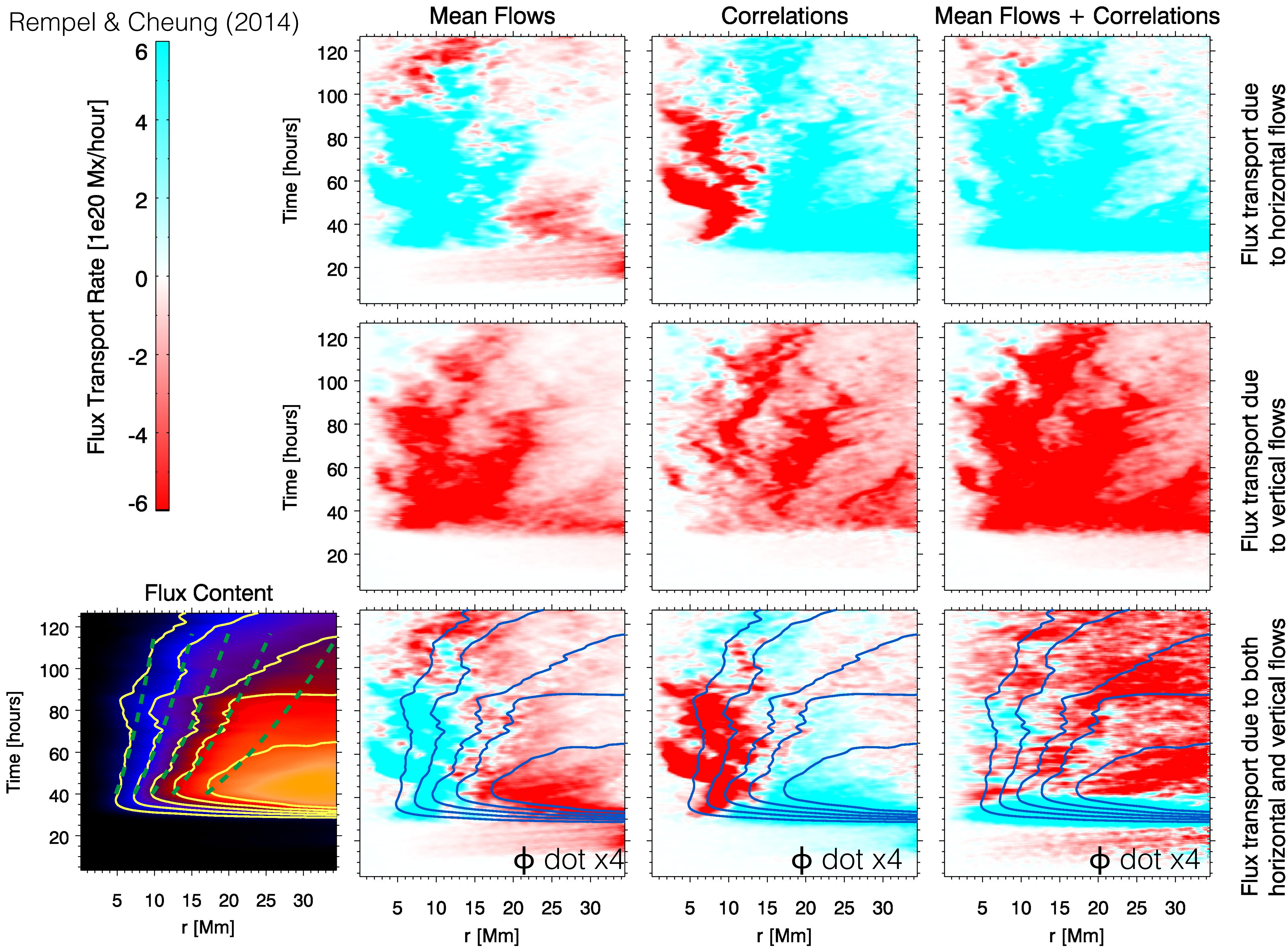

Rempel & Cheung (2014)
Mean Flows
Correlations
Mean Flows + Correlations
Flux Transport Rate [1e20 Mx/hour]
6
4
2
0
-2
-4
-6
Time [hours]
Flux transport due to horizontal flows
Flux transport due to vertical flows
Flux transport due to both horizontal and vertical flows
Flux Content
ϕ dot x4
r [Mm]

Flux Spreading in the Decay Phase

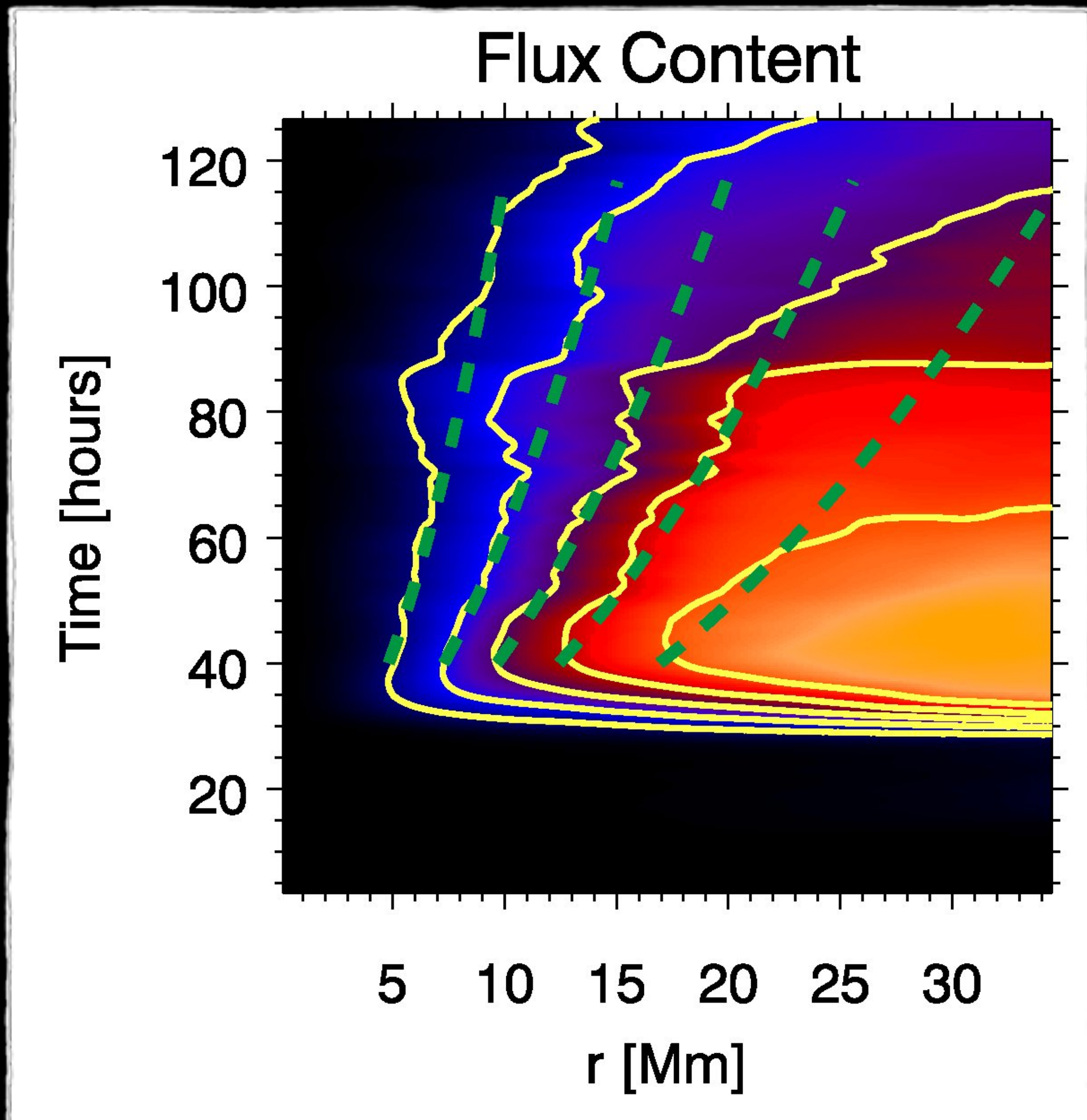

Decay due to turbulent diffusion (see Meyer et al 1974 and Mosher 1977)

$$B_z(r,t) = \frac{\Phi_0}{\pi\sigma(t)^2} e^{-r^2/\sigma(t)^2}, \text{ where}$$

$$\sigma(t) = \sqrt{\sigma_0^2 + 4\eta_{\mathrm{turb}} t}.$$

Green dashed lines show the self-similar solution for:
$\Phi_0 = 1.1 \times 10^{22}$ Mx,
$\sigma_0 = 11$ Mm, and
$\eta_{Turb} = 350\ \mathrm{km^2 s^{-1}}$.

Yellow contours show surfaces of constant enclosed flux in intervals of 2×10^{21} Mx (for the leading polarity).

Convection-driven Emergence

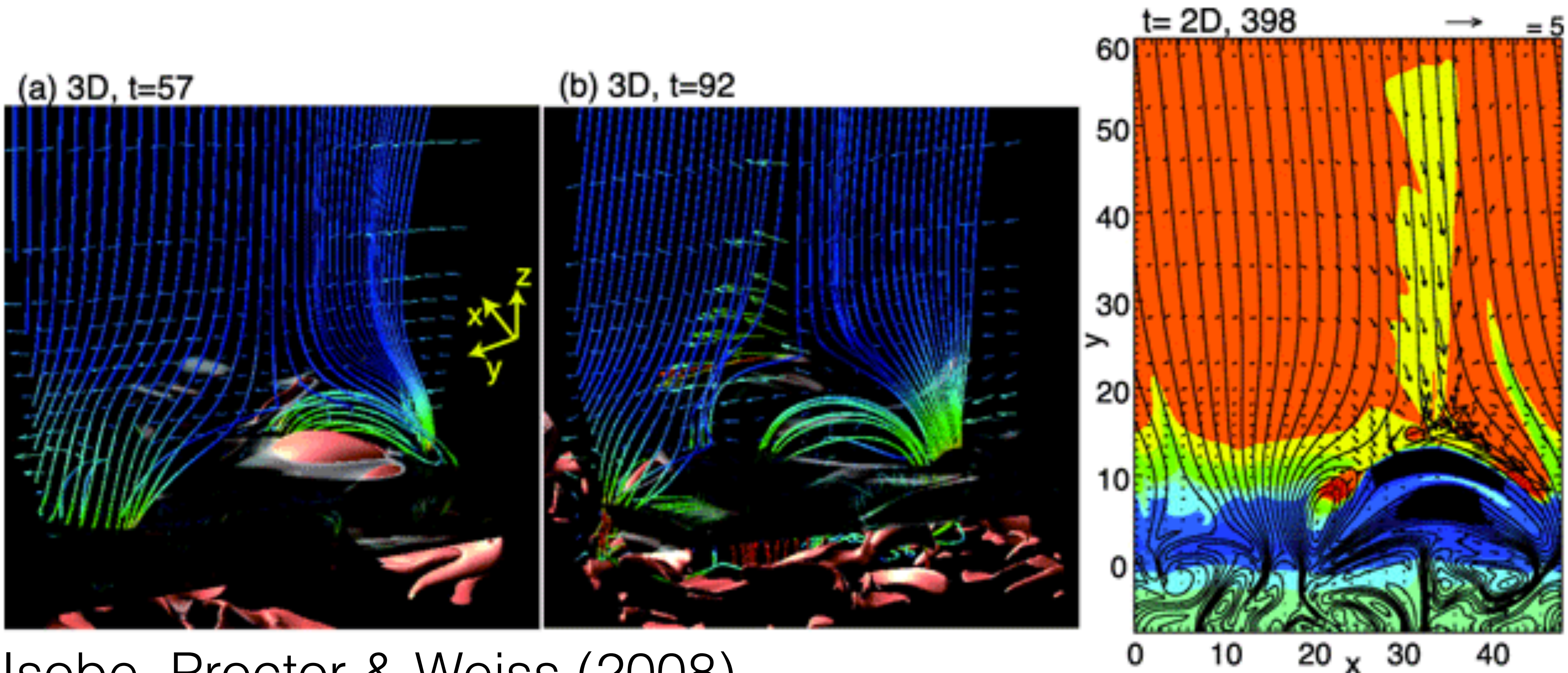

Isobe, Proctor & Weiss (2008)

- Magnetoconvection brings small-scale loops up to the surface, which then reconnect with the surrounding field. This is a source of high-frequency waves in the atmosphere.


Twist

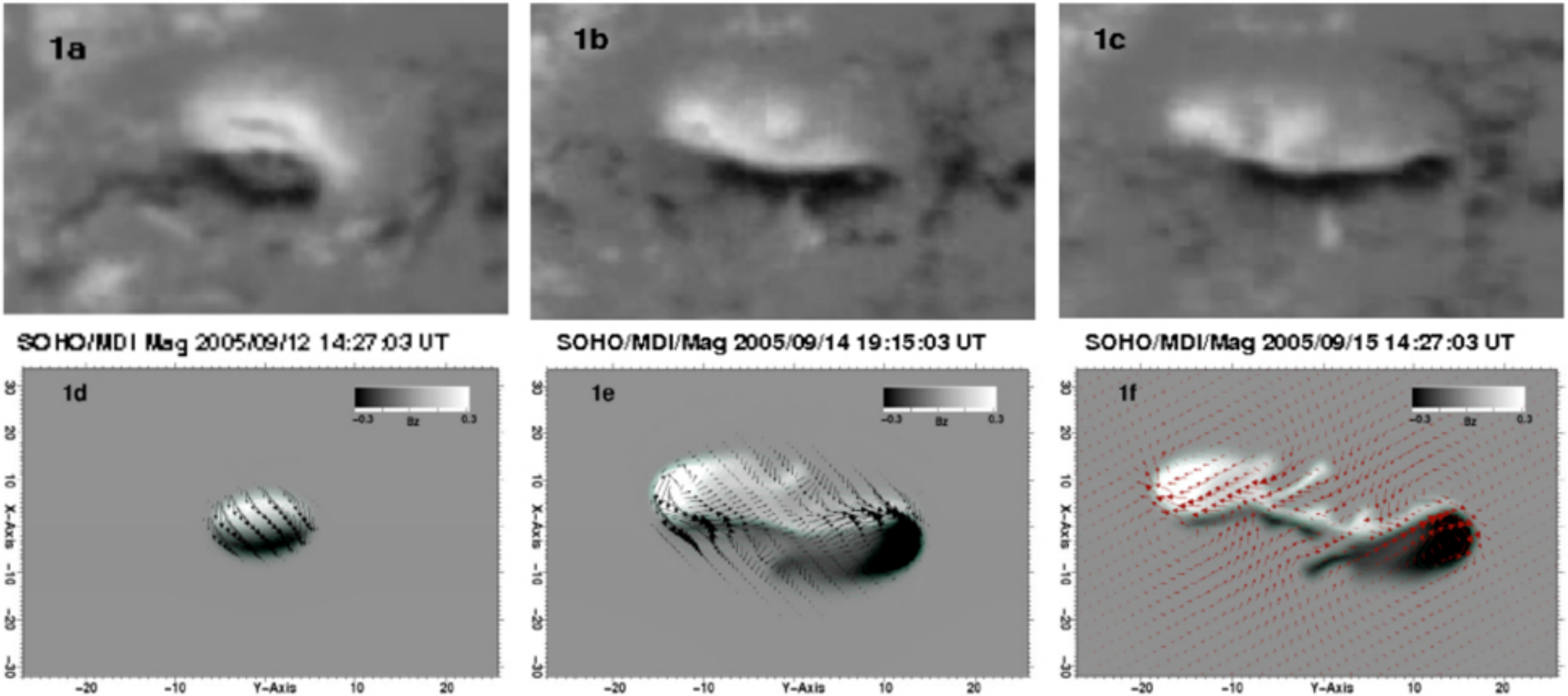

Figure 38: Evidence for twisted flux tube emergence. The top row shows three SoHO/MDI magnetograms of NOAA AR 10808. The positive and negative polarities have 'magnetic tongue' morphology. The bottom row shows three synthetic magnetograms from the simulation of the emergence of a twist flux tube. The striking resemblance in morphology suggests a twisted flux rope structure for NOAA AR 10808. Image reproduced with permission from Archontis and Hood (2010), copyright by ESO.

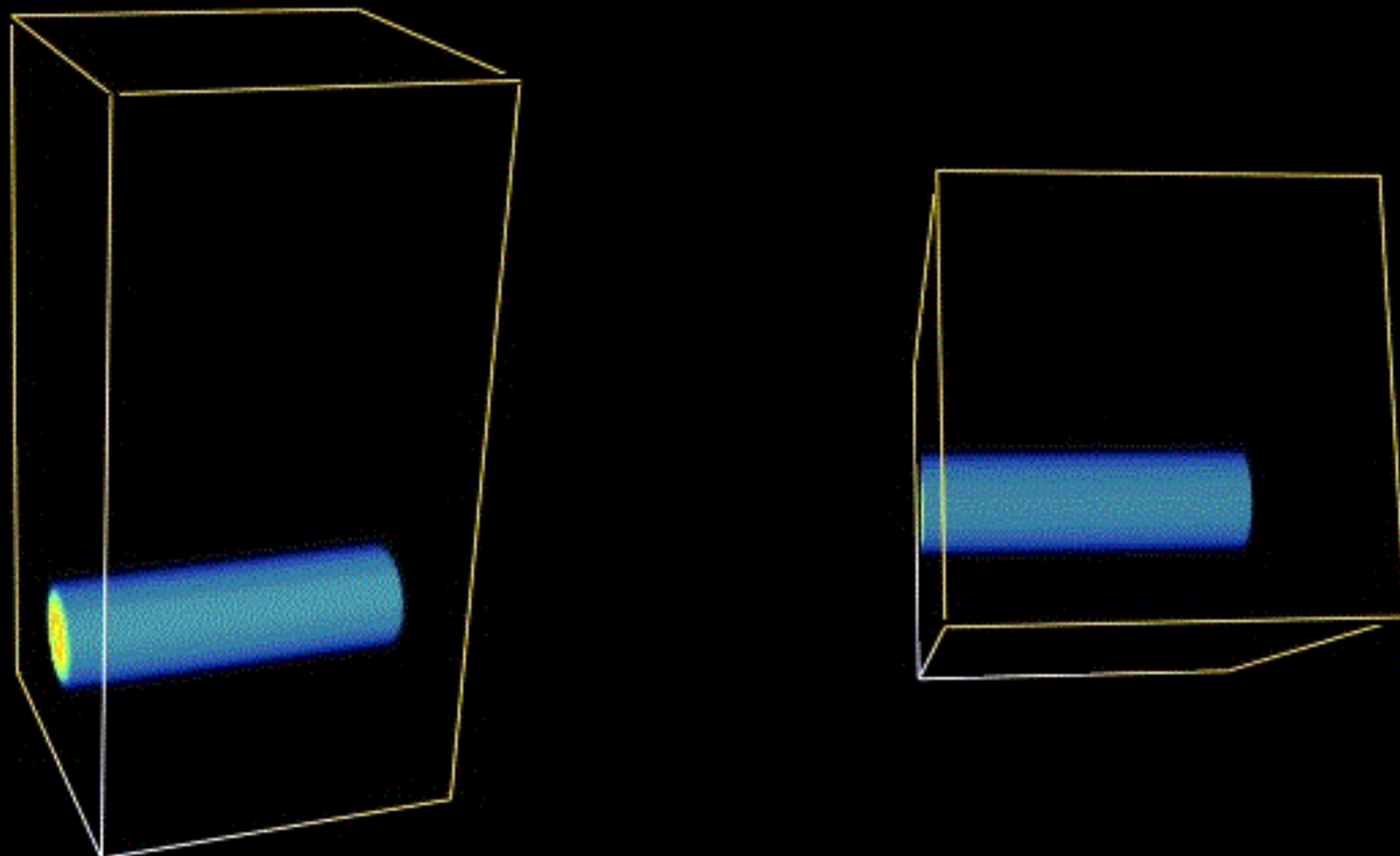

Fan et al. (1999): Non-linear development of the helical kink instability in a buoyant flux tube. See Takasao’s talk for helically kink unstable emerging flux.

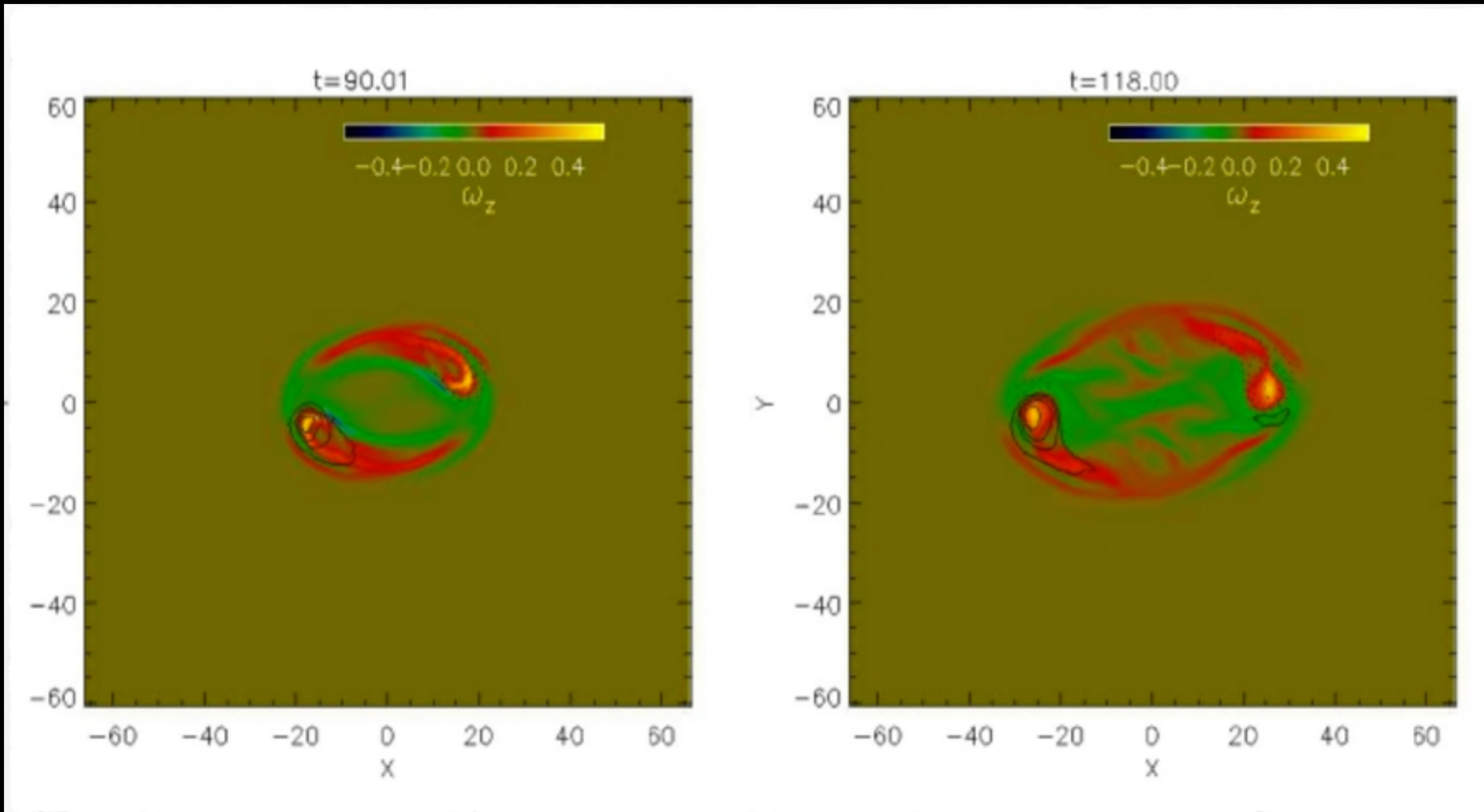

Fan (2009): Distribution of vorticity (vertical component) at the photosphere from a simulation of the emergence of a twisted flux rope. The two ‘spots’ have the same sign of rotation.

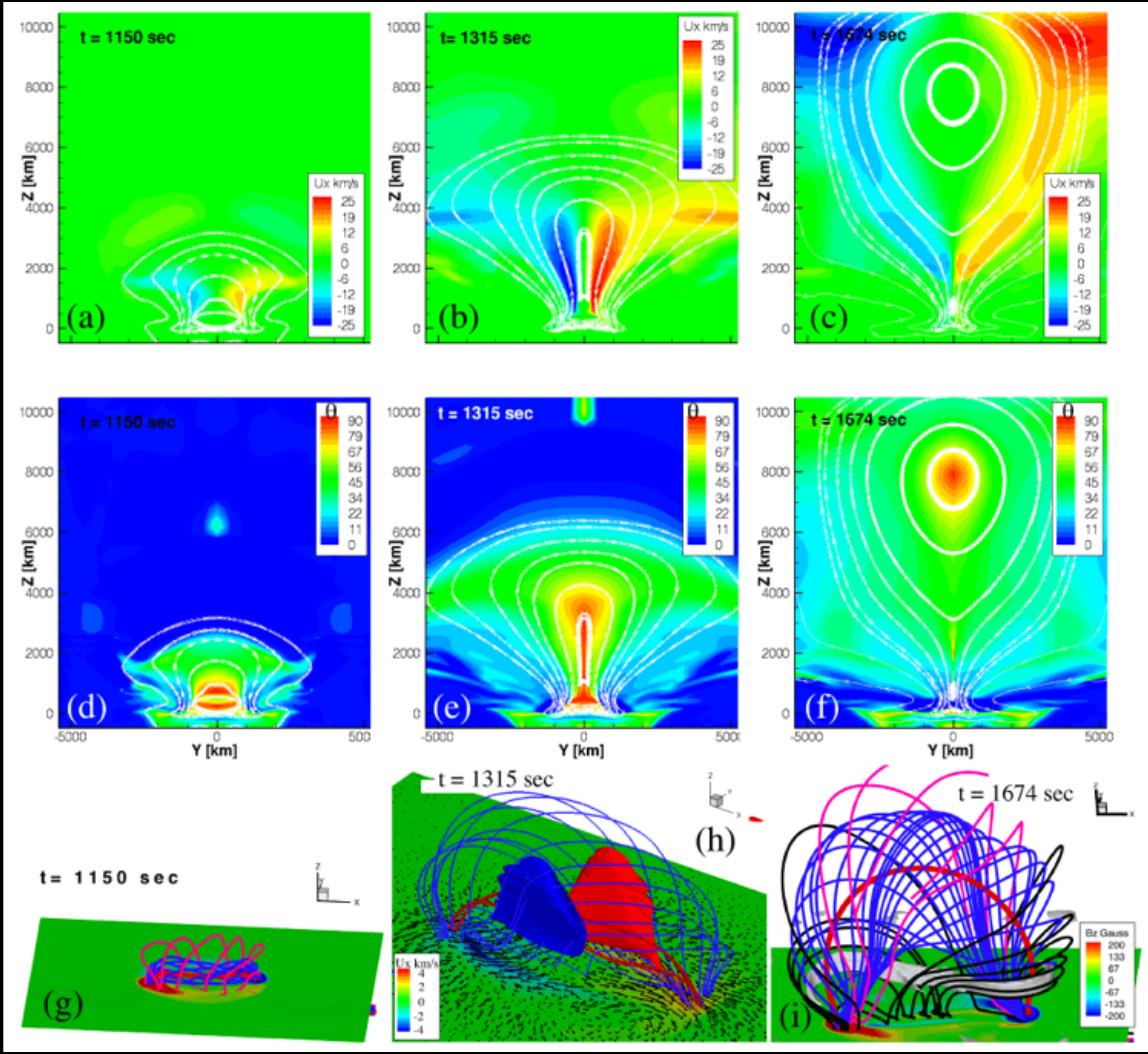

Manchester et al. (2004)

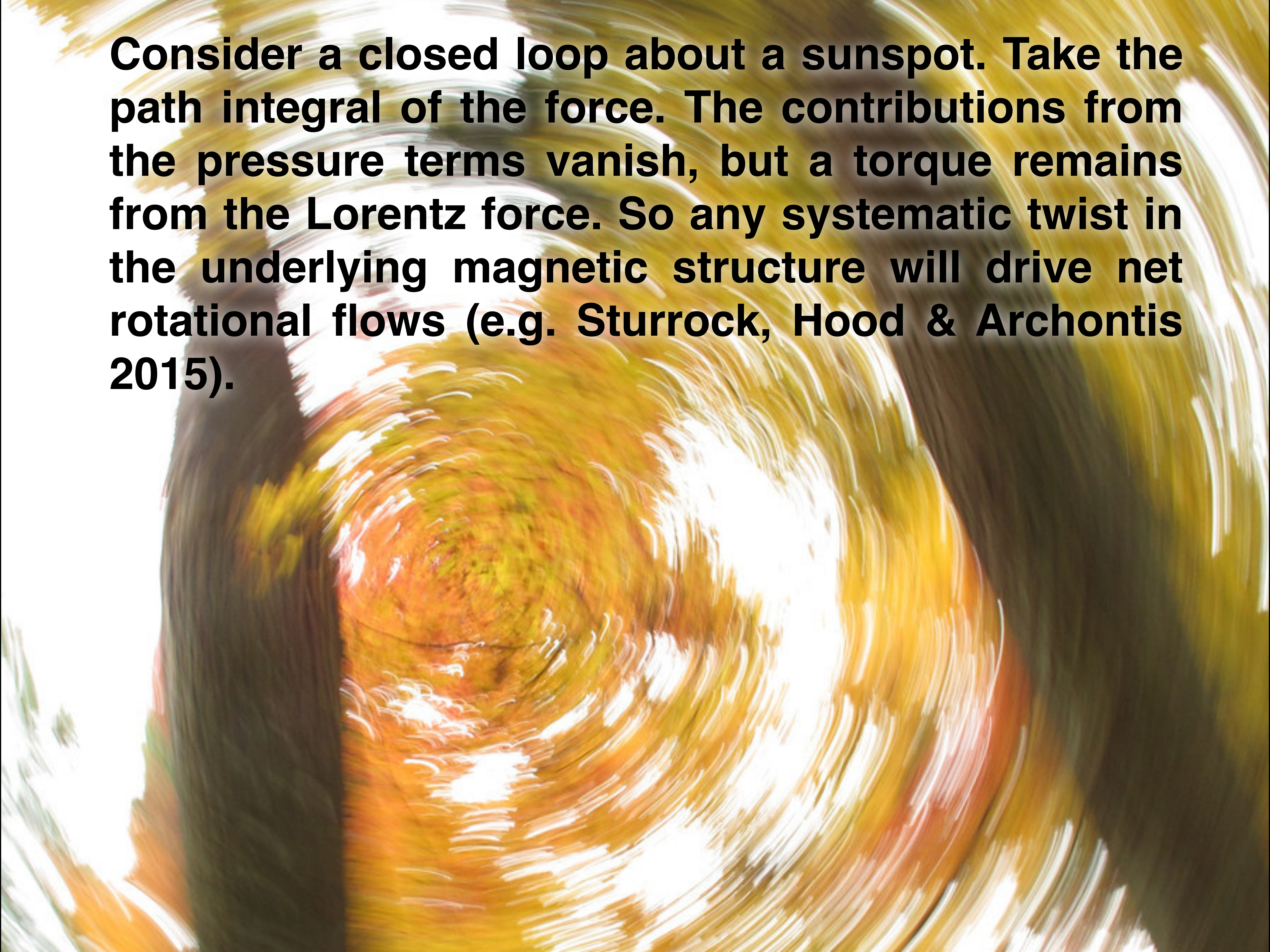

Consider a closed loop about a sunspot. Take the path integral of the force. The contributions from the pressure terms vanish, but a torque remains from the Lorentz force. So any systematic twist in the underlying magnetic structure will drive net rotational flows (e.g. Sturrock, Hood & Archontis 2015).

A Simple Model by Longcope & Welsch (2000)

- "Current shunting" model for twisted active region emergence
- Idealized emerging active region has net twist
- Matched to force-free coronal field
- At the interface (photosphere), a horizontally diverging current drives a torque, which sends a torsional Alfvén wave down the tube.
- Over an Alfvén crossing time ~ 1 day (100 Mm @ 1 km/s), the tube unwinds while the coronal field is twisted up.

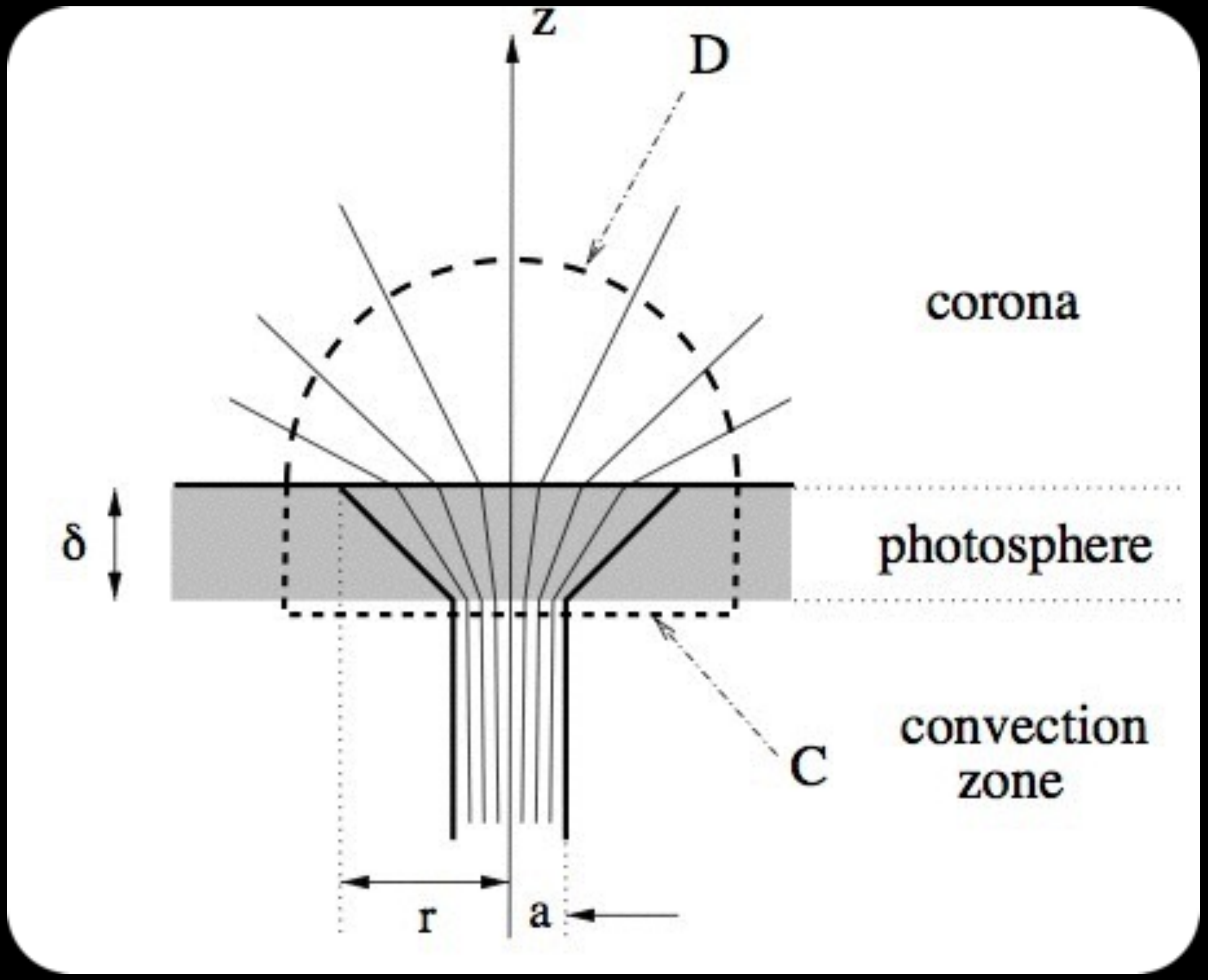

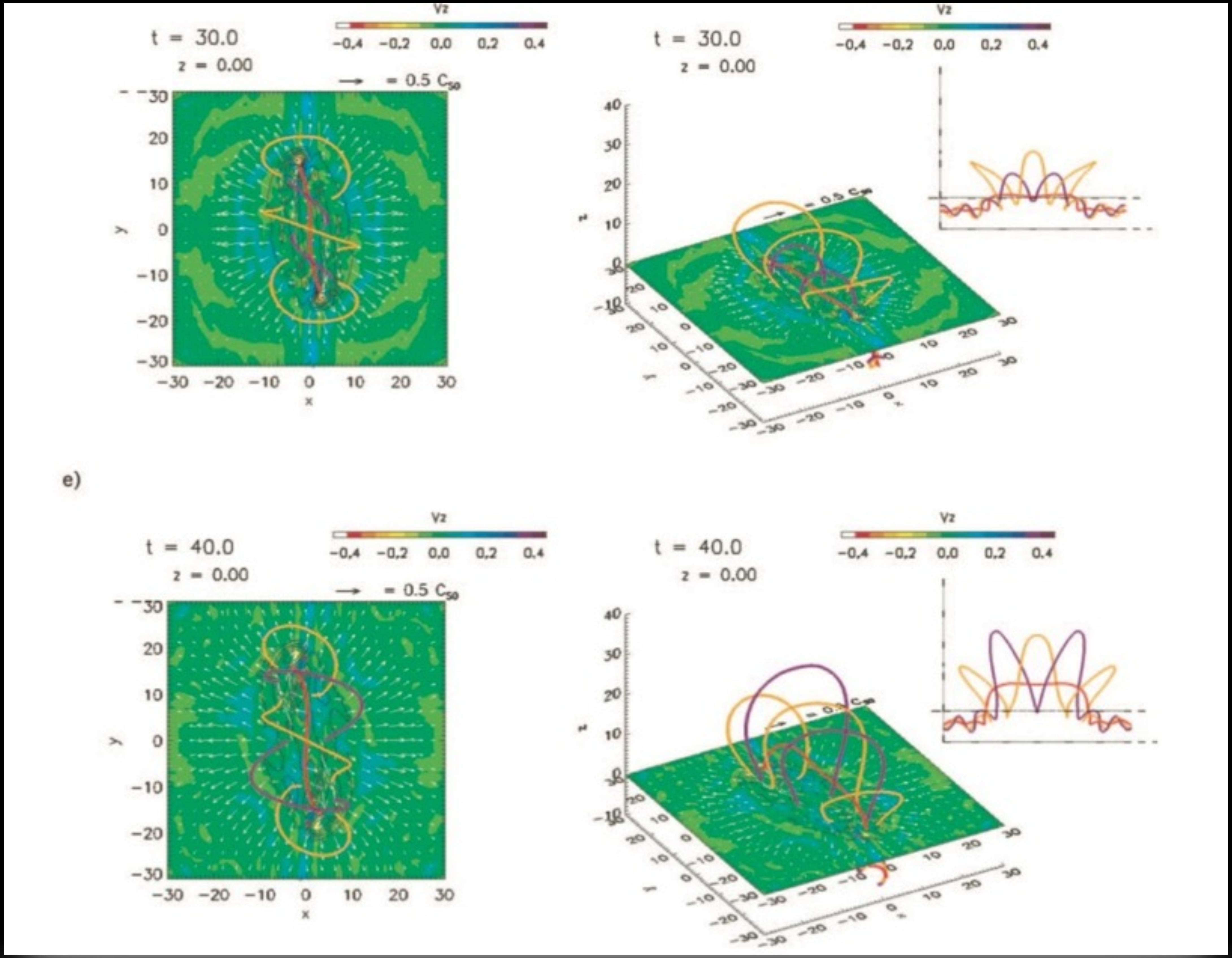

From Magara & Longcope (2003): Poynting fluxes of magnetic energy and relative helicity in a 3D flux emergence simulation. Note how the shear (horizontal motion) contribution outlasts the emergence (vertical motion) contribution.

Origin of Twist?

Still somewhat controversial

- Mean-field Dynamo **α** effect*? Longcope et al. (1999) says it predicts the wrong sign of twist.
- They propose instead the **Σ** Effect: namely an initial flux tube in the solar interior has zero magnetic helicity. Interaction with helical convection introduces writhe of tube axis. Helicity conservation means twist of opposite sign is produced✿.
- What about wrapping of poloidal field lines over a rising flux tube (Choudhuri, Chatterjee & Nandy 2004)?
- Studies of the solar cycle variation of active region twist may put important constraints to reject models. See work of Hagino & Sakurai, M. Zhang, Pevtsov and collaborators. For latest, consult the Space Science Reviews paper by Pevtsov, Berger, Nindos, Norton & van Driel-Gesztelyi (2015).
- Global convective dynamo simulations (e.g. Hotta, Nelson, Fan) that self-consistently generate flux tubes may provide an answer (or tell us it's much more complicated).

*The **α** effect is an EMF parallel to <B> due to turbulence.

✿ But but but … Seehafer (Phys Rev E, 1283, 1996): The **α** effect generates helicity in the small and large scales with equal amplitude but opposite signs!

Ion-neutral interaction

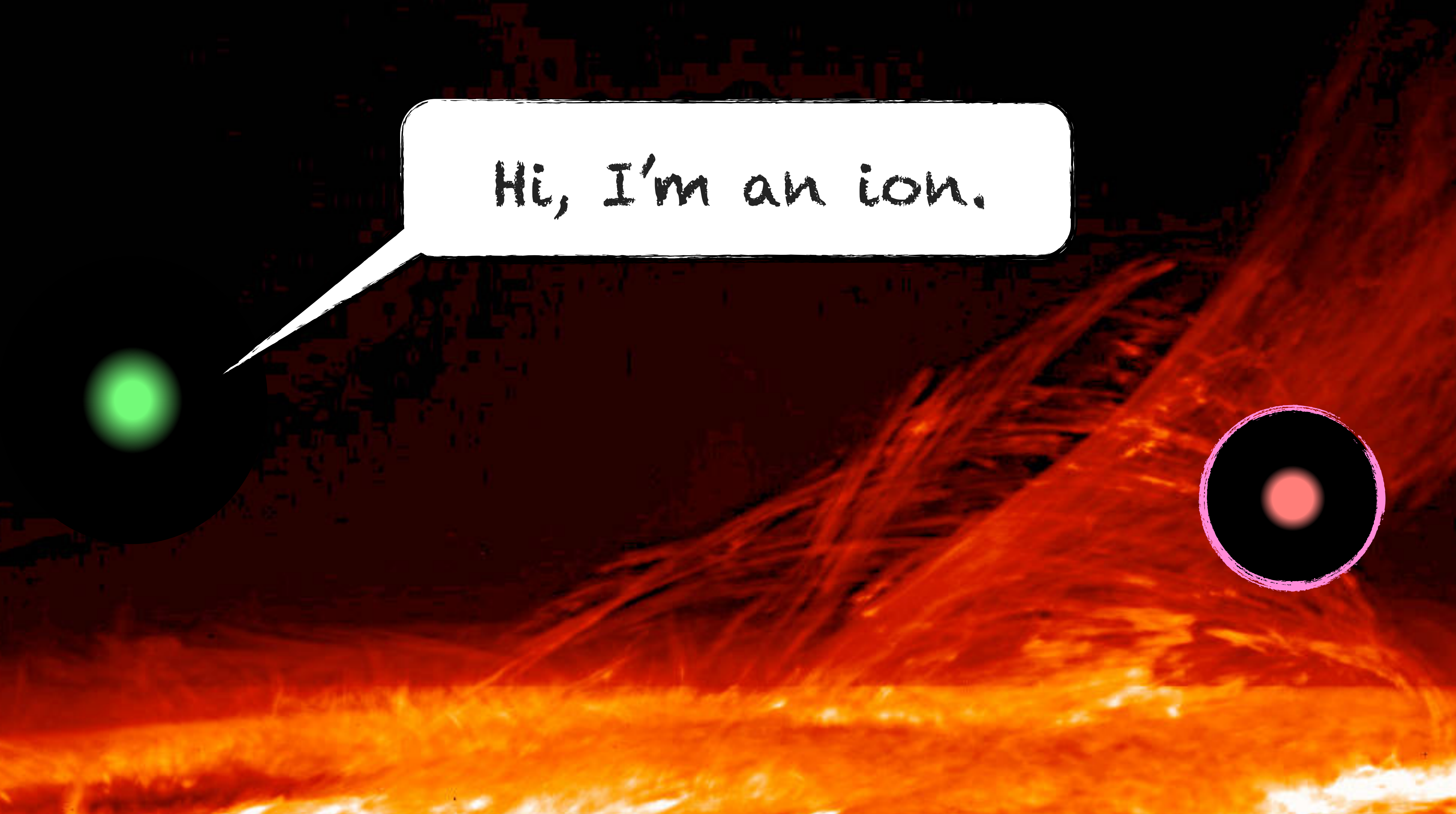

Ion-neutral interaction

Ion-neutral interaction

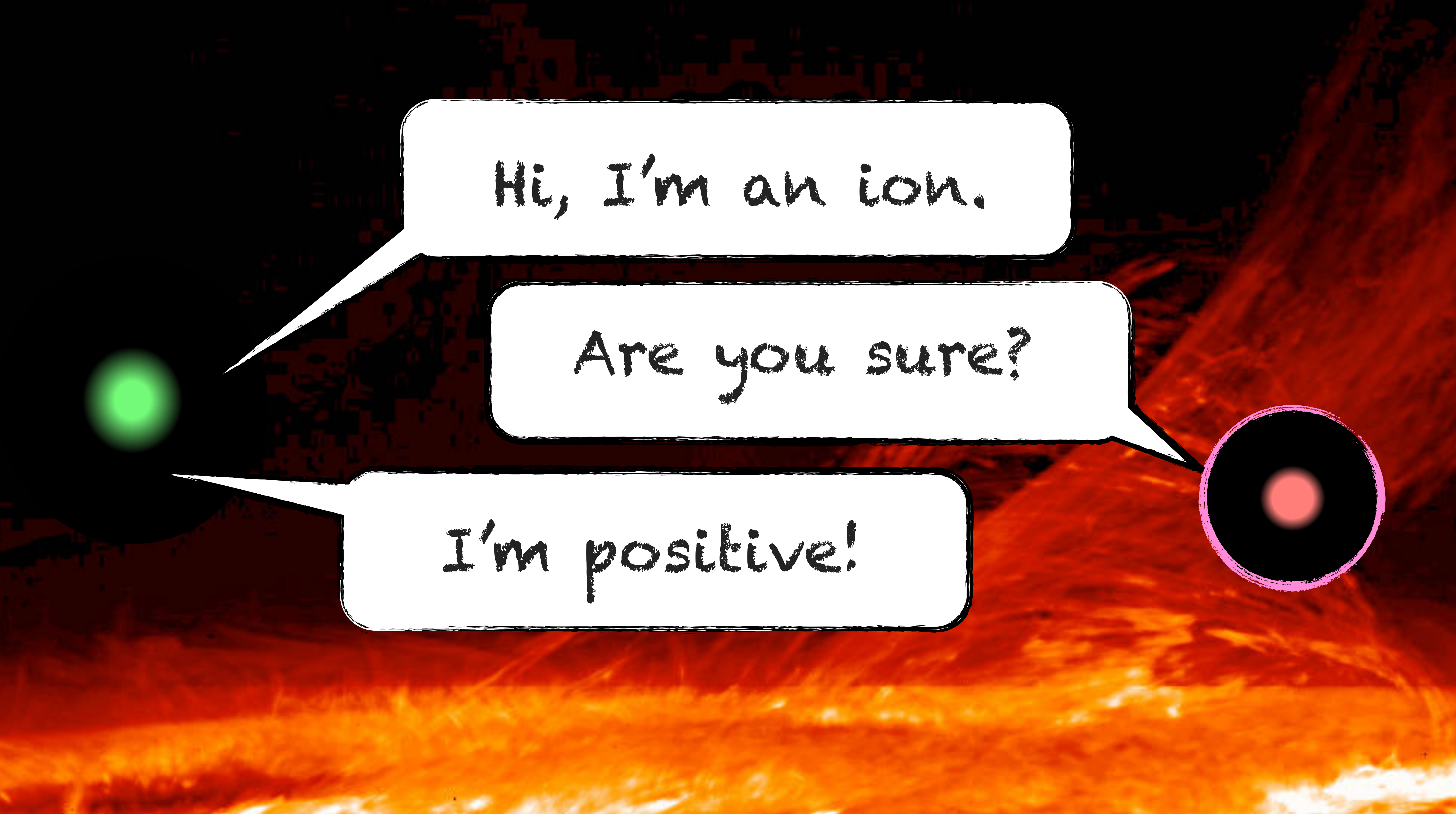

Generalized Ohm's Law

$$\frac{\partial \mathbf{B}}{\partial t} = \nabla \times \left[\mathbf{v} \times \mathbf{B} - \frac{4\pi\eta}{c}\mathbf{j} - \frac{1}{en_e}\mathbf{j} \times \mathbf{B} + (\mathbf{j} \times \mathbf{B}) \times \mathbf{B}\frac{D^2}{c\varrho_i\,\nu_{\rm in}} \right] , \tag{59}$$

where $\mathbf{j} = c(4\pi)^{-1}\nabla \times \mathbf{B}$ is the current density, n_e is the electron number density, ϱ_i is the mass density of the ionized component of the plasma, $D = \varrho_n/(\varrho_i + \varrho_n)$ is the neutral mass fraction, and $\nu_{\rm in}$ is the rate of ion-neutral collisions. The first and second terms inside the bracket on the r.h.s.

$$\frac{\partial \mathbf{B}}{\partial t} = \nabla \times \left[\mathbf{u} \times \mathbf{B} - \frac{4\pi}{c}\eta\mathbf{j} \right] , \tag{60}$$

where

$$\mathbf{u} = \mathbf{v} + \mathbf{v}_{\rm Hall} + \mathbf{v}_{\rm Amb} \,, \tag{61}$$

$$\mathbf{v}_{\rm Hall} = -H\nabla \times \mathbf{B} \,, \tag{62}$$

$$\mathbf{v}_{\rm Amb} = M(\nabla \times \mathbf{B}) \times \mathbf{B} \,, \tag{63}$$

$$H = \frac{c}{4\pi e n_e} \,, \tag{64}$$

$$M = \frac{D^2}{4\pi\varrho_i\nu_{\rm in}} \,. \tag{65}$$

Physical effects of Ohm's Law

	Fluid Motion Induction	Ohmic Diffusion	Hall Effect	Ambipolar Diffusion
Of the form $-E=v^{*}xB$?	Yes / u	No	Yes / j	Yes / jxB
Changes topology?	No	Yes	No	No
Dissipative ?	No	Yes	No	Yes

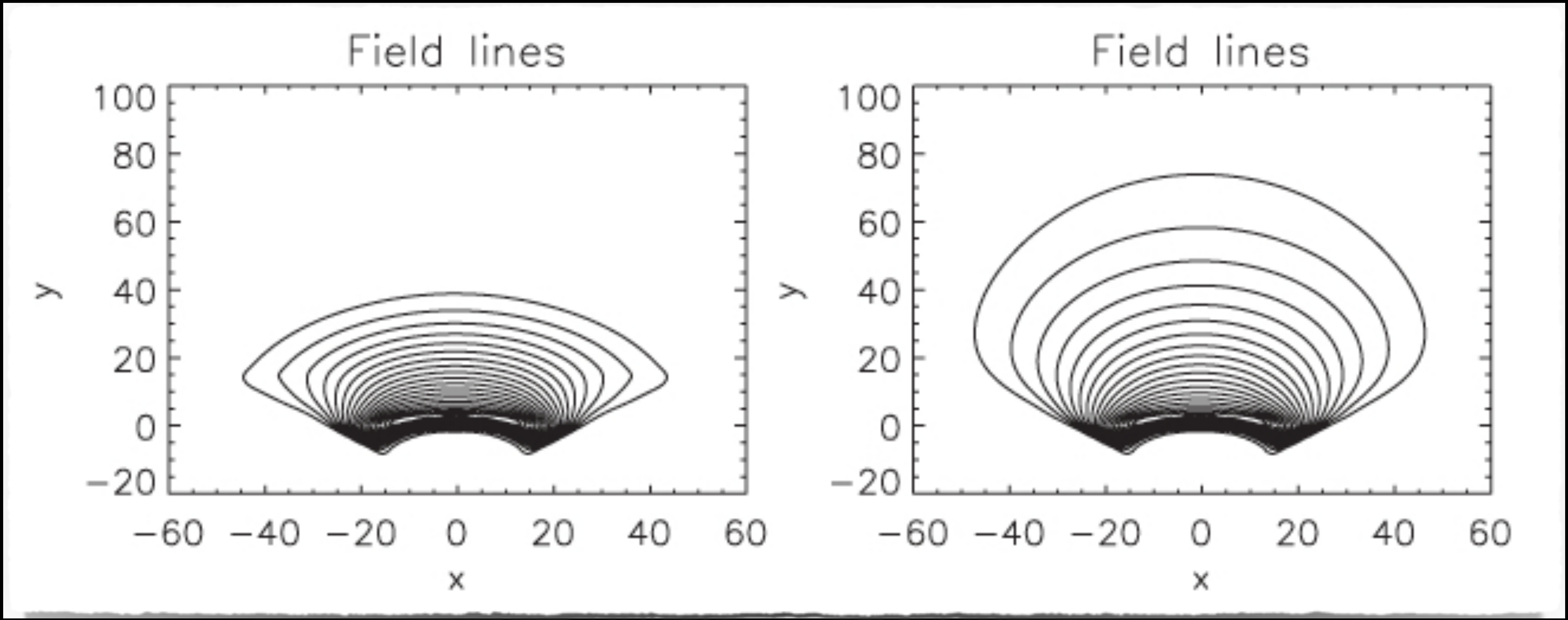

Leake & Arber (2006): Inclusion of the Cowling resistivity (i.e. Ohmic + ambipolar) leads to increased rate of flux emergence (right). The emerged field is also more force-free.

However, they used a simplified 1D prescription for the ionization degree of hydrogen. For (more) self-consistent simulations investigating the effect the ambipolar effect in the solar atmosphere, refer to Juan's papers. (Time-dependent H-ionization?)

Interaction with pre-existing field

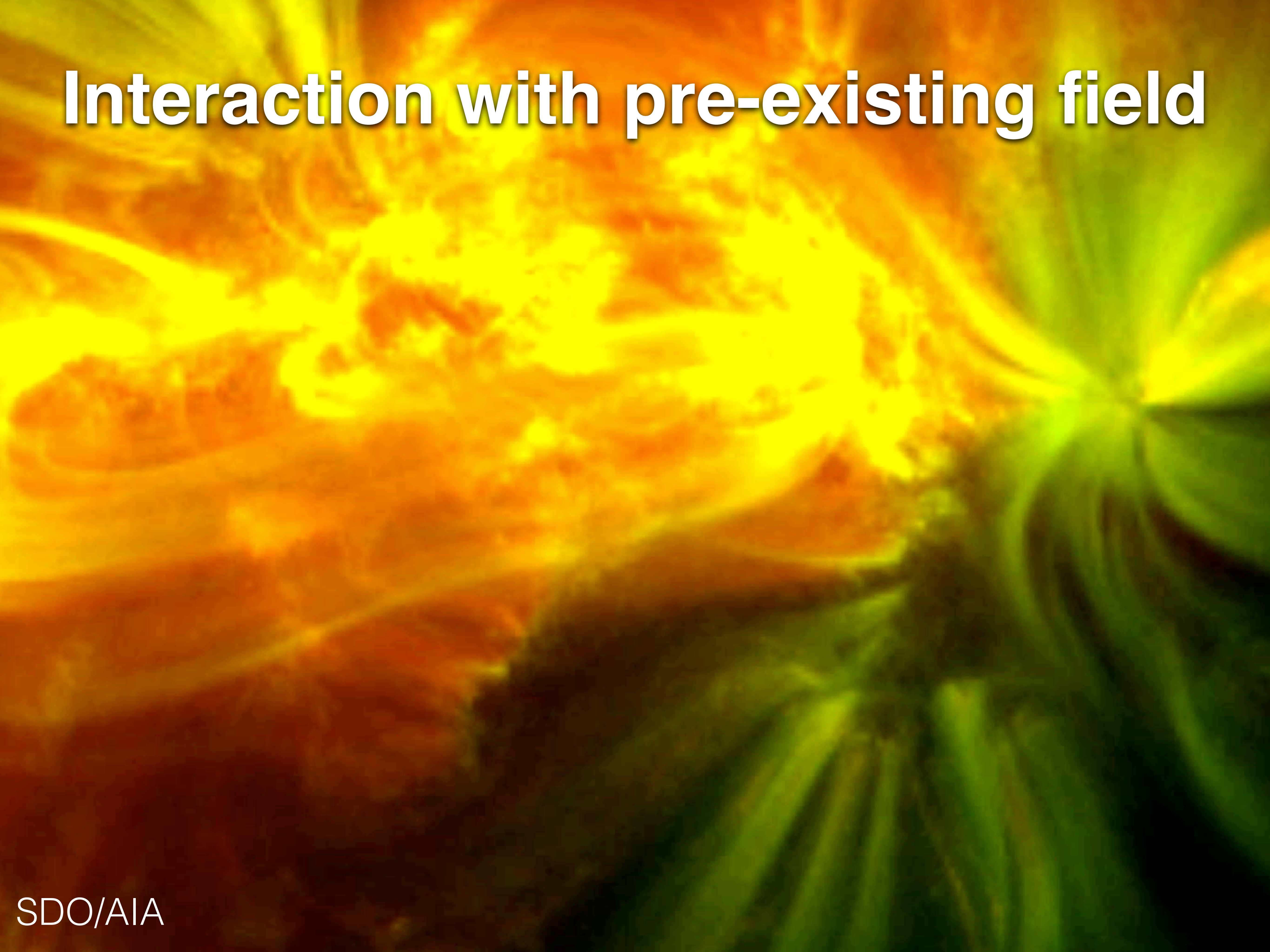

SDO/AIA

Interaction with pre-existing field

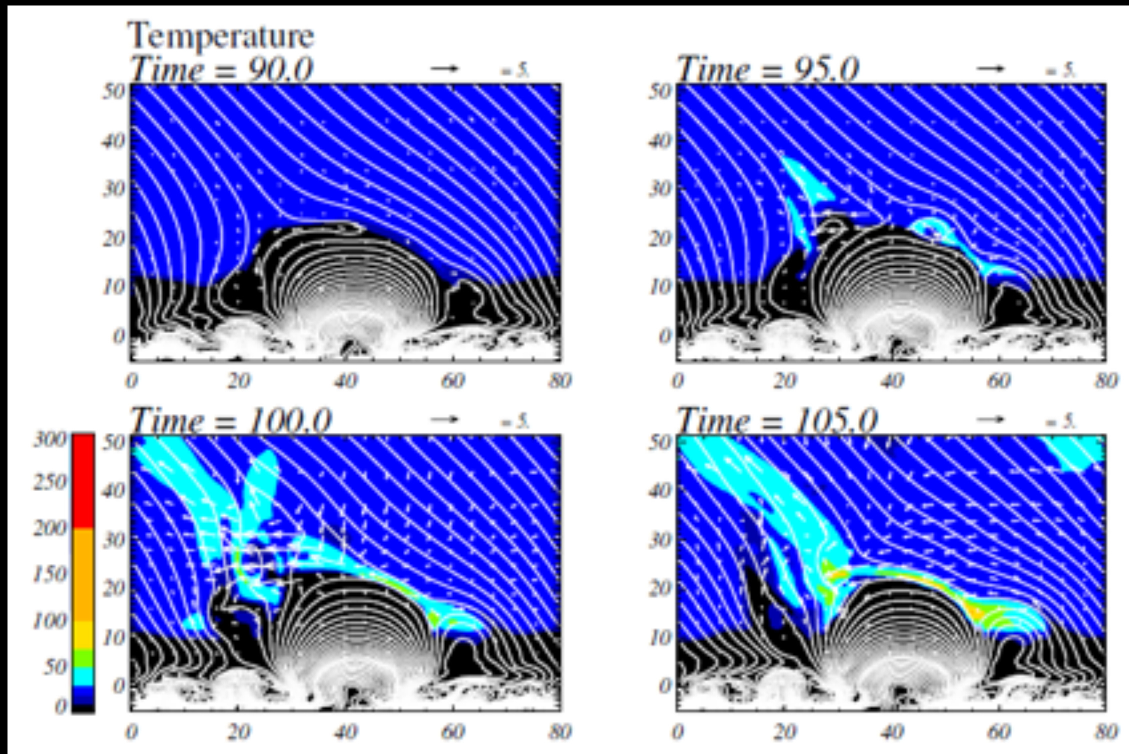

Yokoyama & Shibata (1996): 2D MHD simulation of current sheet formation, leading to plasmoid ejections

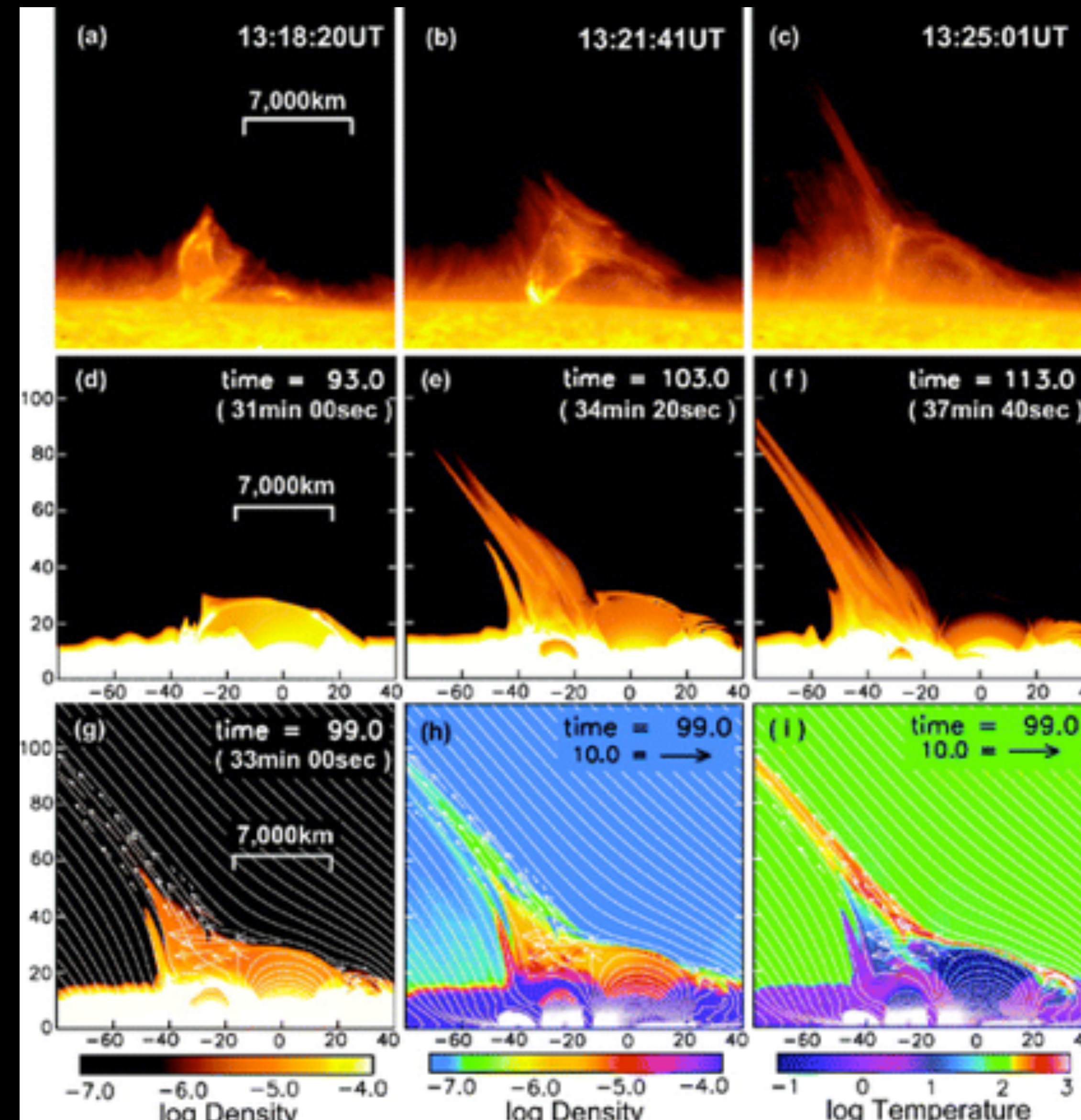

Nishizuka et al. (2008):
Alfvén wave generation in jet simulation

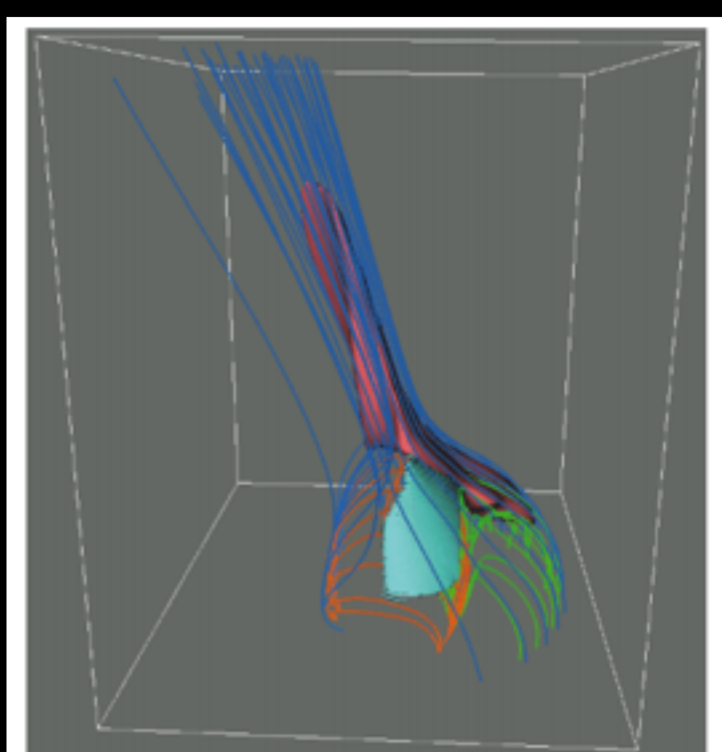

Moreno-Insertis et al. (2008):
3D jet simulation from flux emergence into a coronal hole

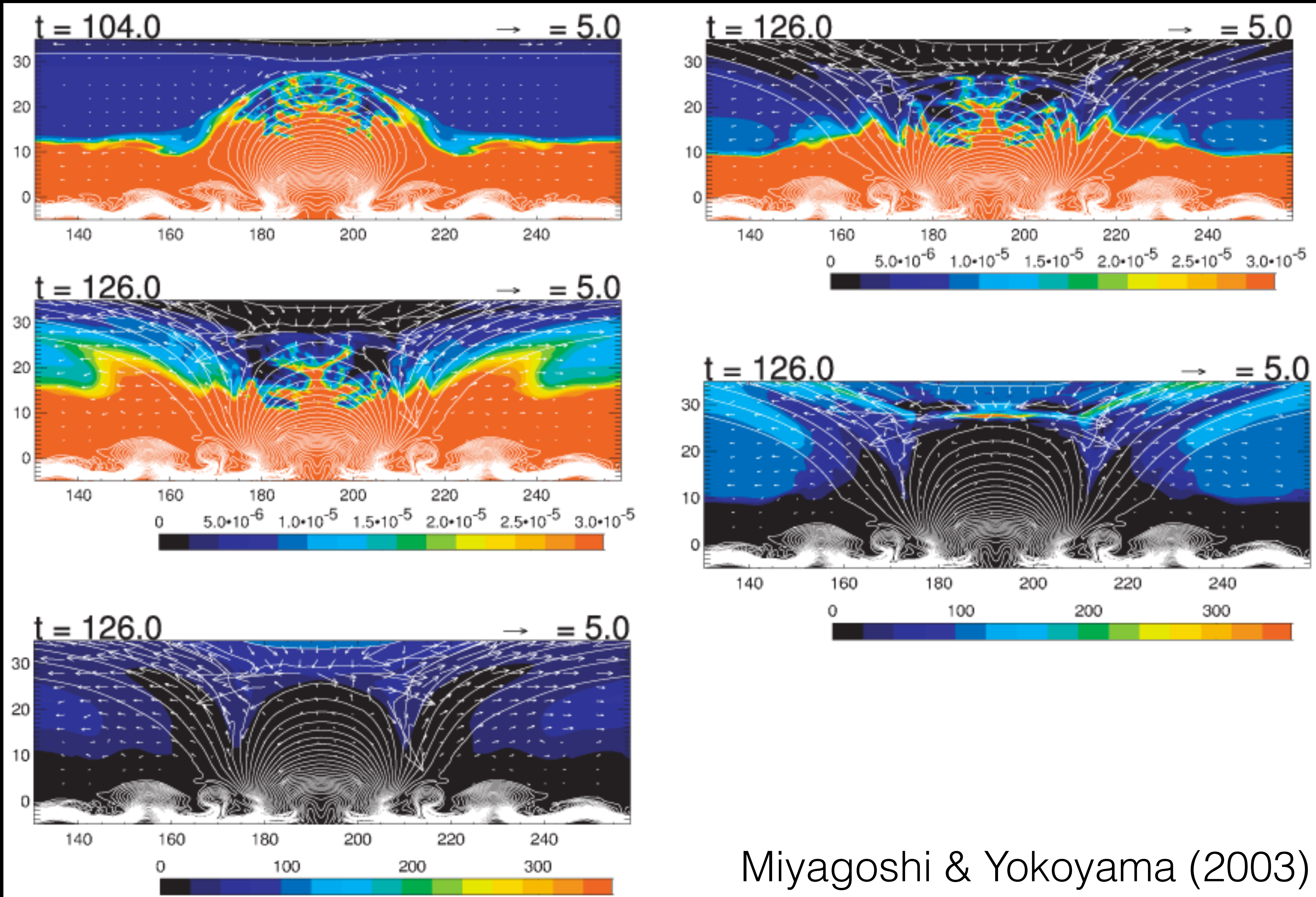

Left: with anisotropic thermal conduction

Right: without anisotropic conduction


Data-Driven Modeling

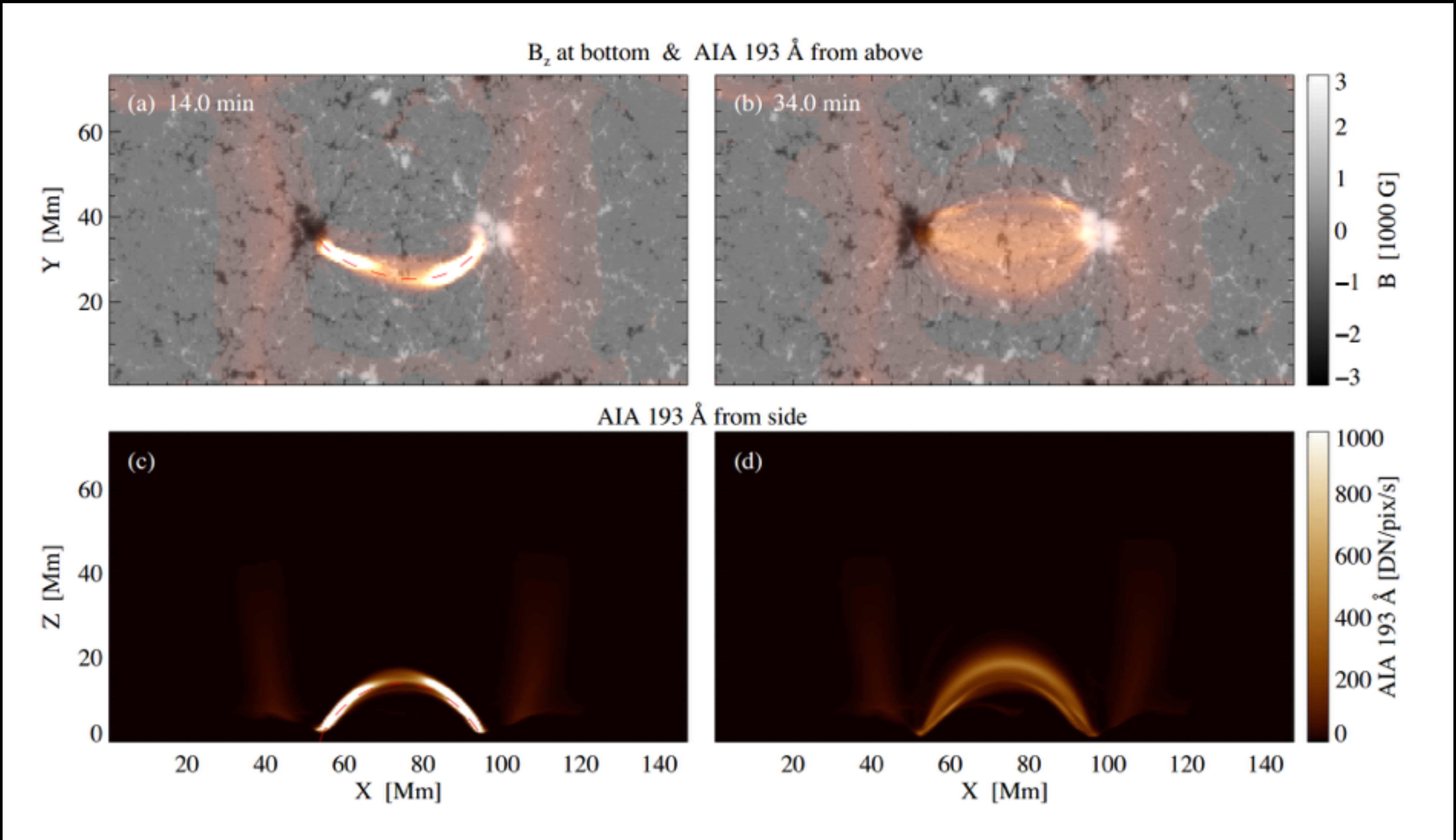

Chen et al. (2014): Simulation of AR corona formation. The simulation includes anisotropic thermal conduction and is driven at the bottom boundary by a model from Rempel & Cheung (2014).

What we need for real data-driven models

Retrieval of electric fields. E-fields of interest at the photosphere cannot be directly measured with remote sensing. It rises from a combination of effects:

- -v x B
- Non-ideal parallel E-fields
- Mean-field EMFs arising from correlations at small scales (- <v'xB'>)
- Finite spatio-temporal resolution and sampling (gives rise to averaging)

Example problems:

a. Retrieve the E-field needed for driving (surface) flux transport models to study the solar cycle (dynamo)

b. Retrieve the E-field integrated along the solar equator

c. To measure the full Poynting flux for magnetic energy and helicity

Hi-fidelity, validated methods for reliable retrieval of photospheric driving E-fields are needed. This is in the works thanks to a number of efforts involving Fisher, Kazachenko, Welsch, Fan, Rempel, Cheung, Linton, Yeates, Peter, Feng; this is not an exhaustive list).

Electric field and Poynting Flux

The formula for the time evolution of H_{rel} (Berger & Field, 1984; Demoulin & Berger (2003) has many terms. Usually only two terms (blue + red) are included by helicity practitioners.

$$
\begin{aligned}
\frac{\mathrm{d}H}{\mathrm{d}t} &= 2\int_S \mathbf{A}_P \times (\mathbf{v}\times\mathbf{B})\cdot\hat{n}\,\mathrm{d}S + \left.\frac{\mathrm{d}H}{\mathrm{d}t}\right|_{\mathrm{dis.}} \\
&= \left.\frac{\mathrm{d}H}{\mathrm{d}t}\right|_t + \left.\frac{\mathrm{d}H}{\mathrm{d}t}\right|_n + \left.\frac{\mathrm{d}H}{\mathrm{d}t}\right|_{So} + \left.\frac{\mathrm{d}H}{\mathrm{d}t}\right|_{\mathrm{dis.}}
\end{aligned}
$$

Volumetric dissipation term

Photospheric flux due to horizontal motions (a.k.a. shearing term)

$$\left.\frac{\mathrm{d}H}{\mathrm{d}t}\right|_t = -2\int_{Sp} (\mathbf{A}_P\cdot\mathbf{v}_t)B_n\,\mathrm{d}S\,,$$

Flux through non-photospheric boundary

$$\left.\frac{\mathrm{d}H}{\mathrm{d}t}\right|_n = +2\int_{Sp} (\mathbf{A}_P\cdot\mathbf{B}_t)v_n\,\mathrm{d}S\,.$$

Photospheric flux due to vertical motions (a.k.a. emergence term)

vxB should really be replaced by ***-E*** (e.g. Kazachenko et al. 2014).

Data-Driven Modeling with Magnetofriction

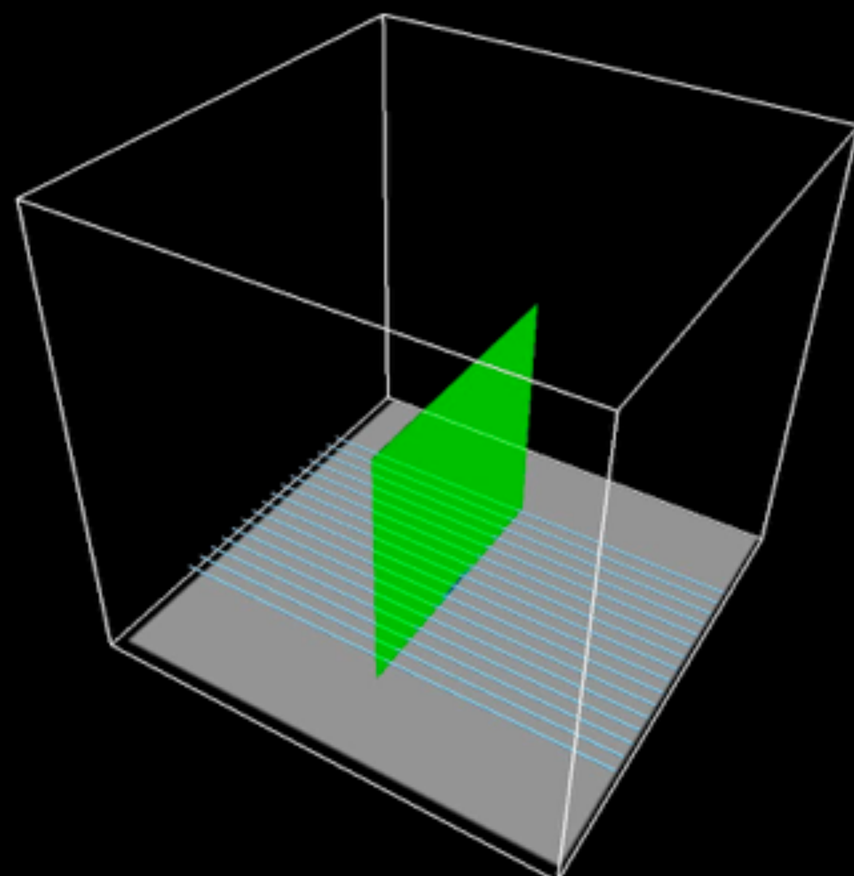

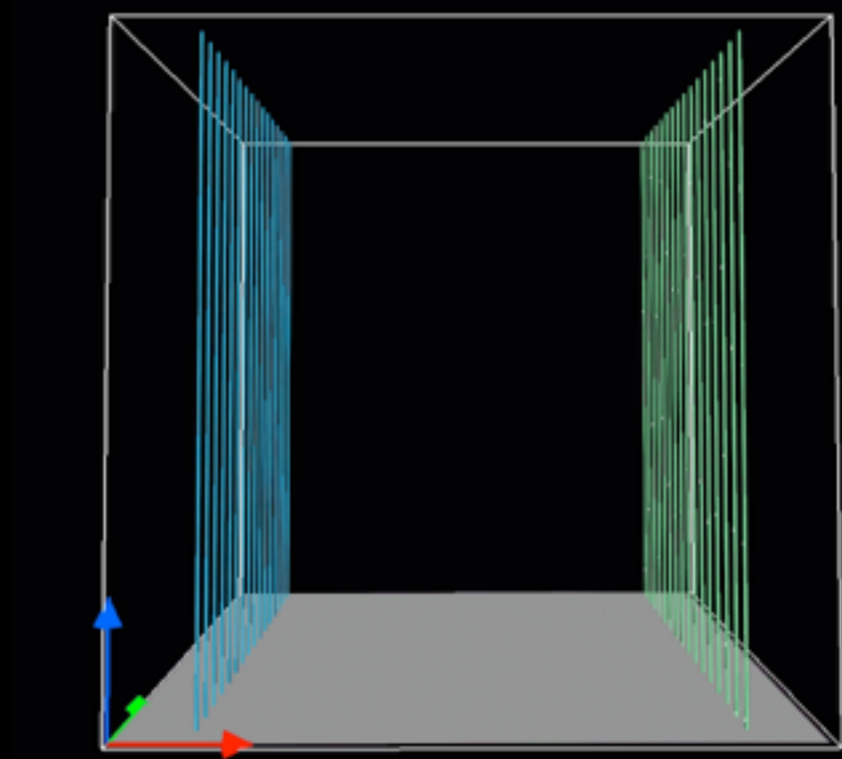

- Balance of Lorentz force and fictitious frictional force (Yang, Sturrock & Antiochos, 1986; Craig & Sneyd 1986)
  - Plasma velocity proportional to Lorentz force: $\boldsymbol{v} = \nu^{-1}\, \boldsymbol{j} \times \boldsymbol{B}$ where ν is the frictional coefficient
  - Evolve magnetic field according to Induction Equation
- Total magnetic energy in volume monotonically decreasing (provided net Poynting flux through boundaries is zero).

Data-Driven Modeling with Magnetofriction

- Van Ballegooijen, Priest & Mackay (2000)
  - Evolve vector potential ***A***
  - Plasma velocity proportional to Lorentz force: $\boldsymbol{v} = (\nu_0 B^2)^{-1} \boldsymbol{j} \times \boldsymbol{B}$
- Yeates, Mackay & Van Ballegooijen (2008)
  - Global magnetofrictional model of coronal field in response to observed changes in photospheric field, including
    - Differential rotation, meridional circulation
    - Flux dispersal and cancellation
    - Appearance of AR-scale, twisted bipoles
  - Correctly reproduces filament chirality and location
  - Memory of corona ~ 6 weeks to a few months

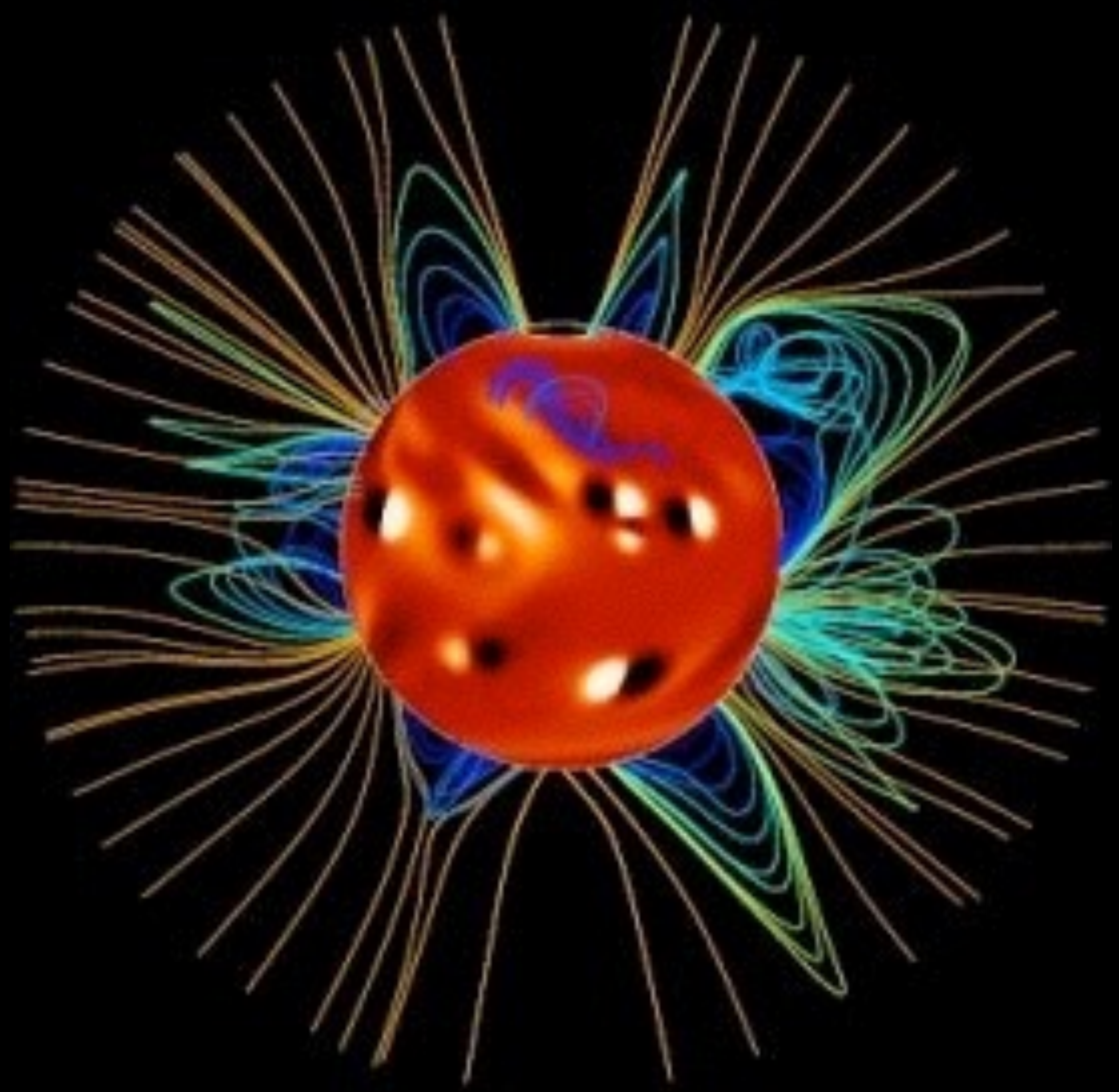

Yeates, Mackay & Van Ballegooijen 2008
See also Yeates 2013

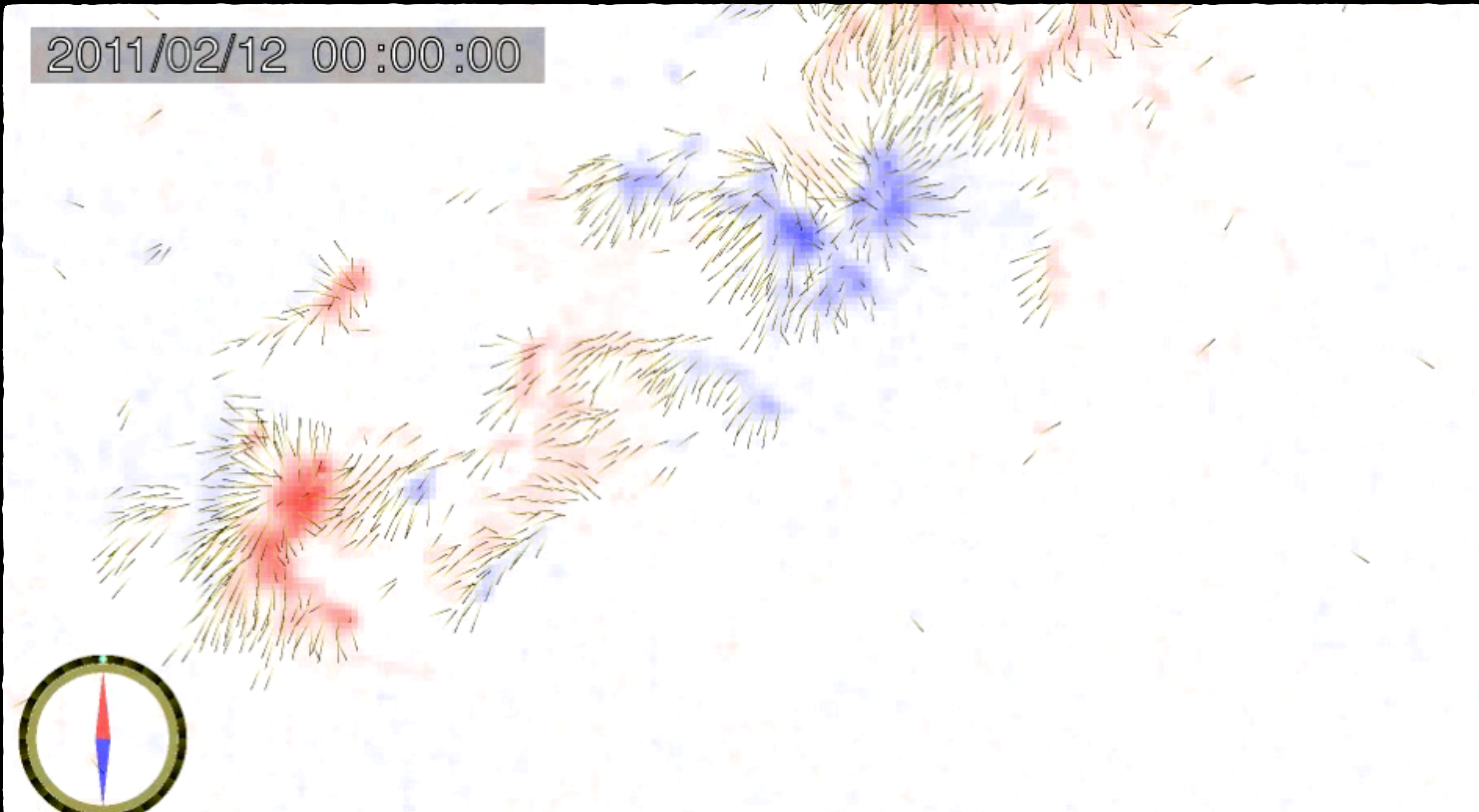

Credit: Keiji Hayashi

Data-Driven model of AR 11158

- CGEM* project: Fisher et al. 2015, Space Weather, 13.
- Electric field boundary condition from inversions by UC Berkeley SSL group (see Kazachenko et al. 2014) with support from Stanford group (Sun, Liu & Hoeksema).
- Magnetofriction model (Cheung & DeRosa) of the evolution of NOAA AR 11158 over 5+ days.

*CGEM is funded by the NASA/NSF Strategic Capability program

Magnetograms at different heights

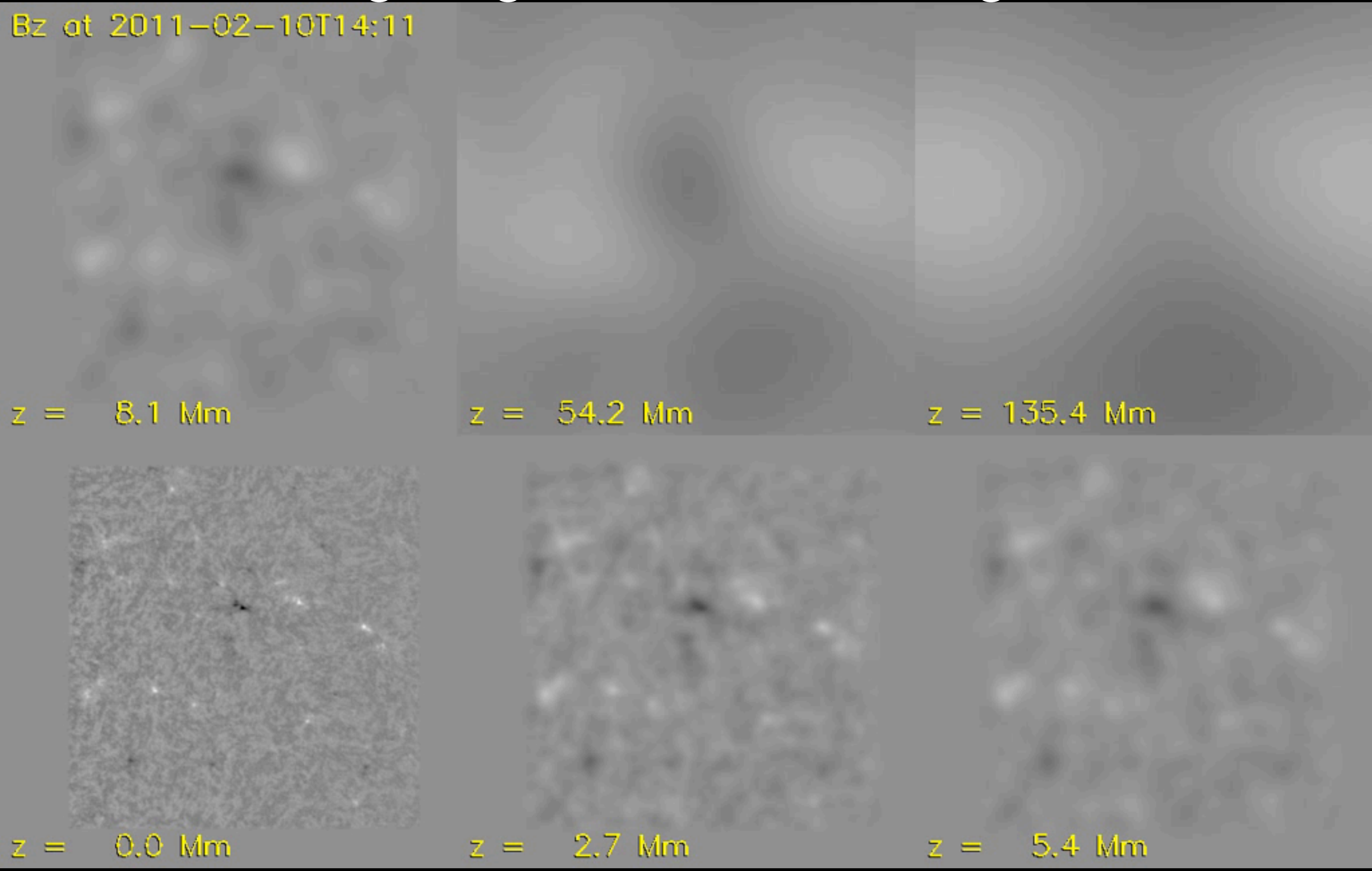

Visualization of field lines based on current density

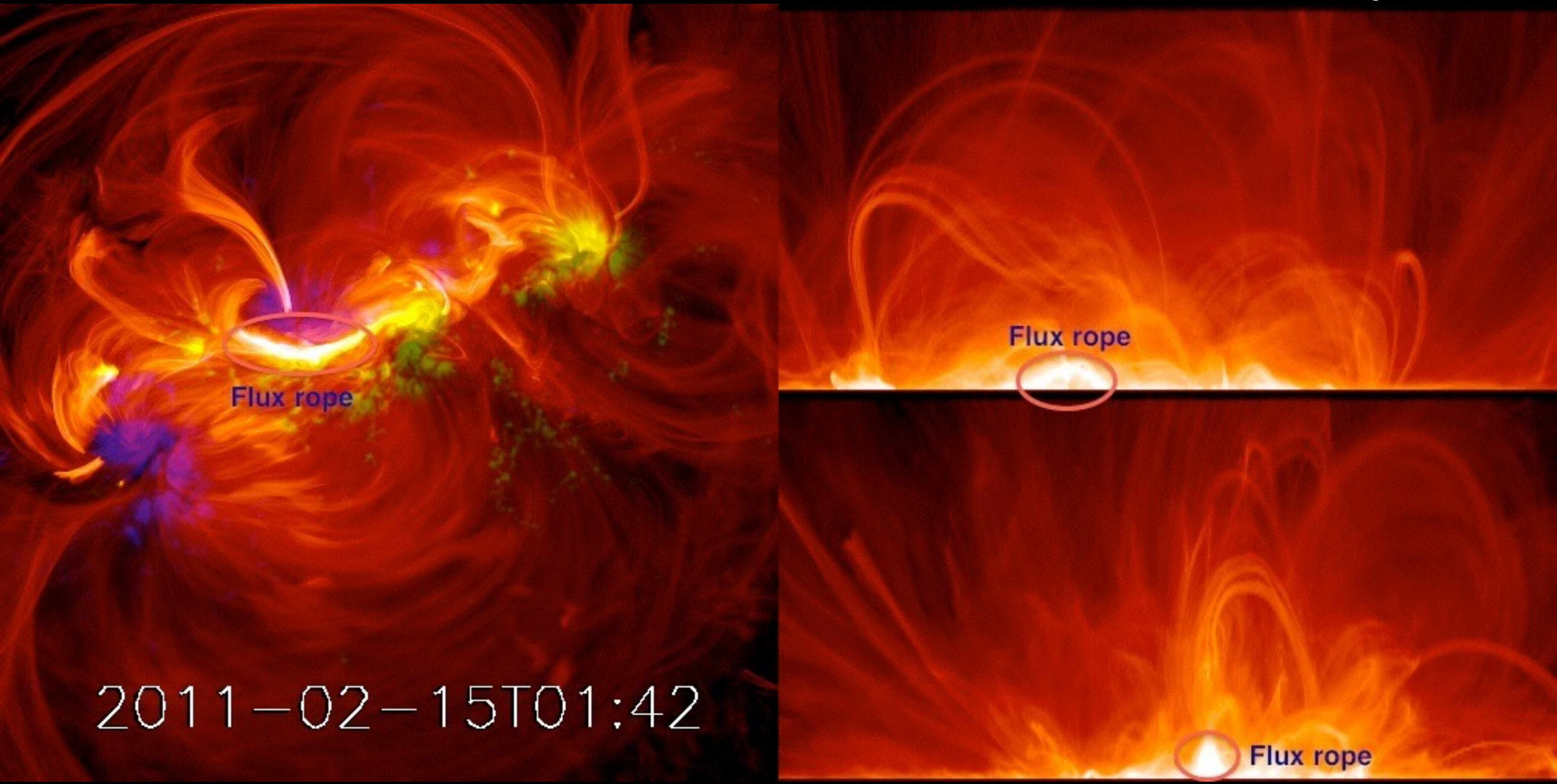

- There is no impulsive eruption at the time of the observed X-flare. However, moments before this time, a current-carrying flux rope is observed to form and is eventually ejected, though the rise time is on the order of hours.
- An extension of this work is to use the destabilized configuration as the initial condition for a MHD run using RADMHD (in progress by Abbett & Bercik).

A Diversity of MHD Models

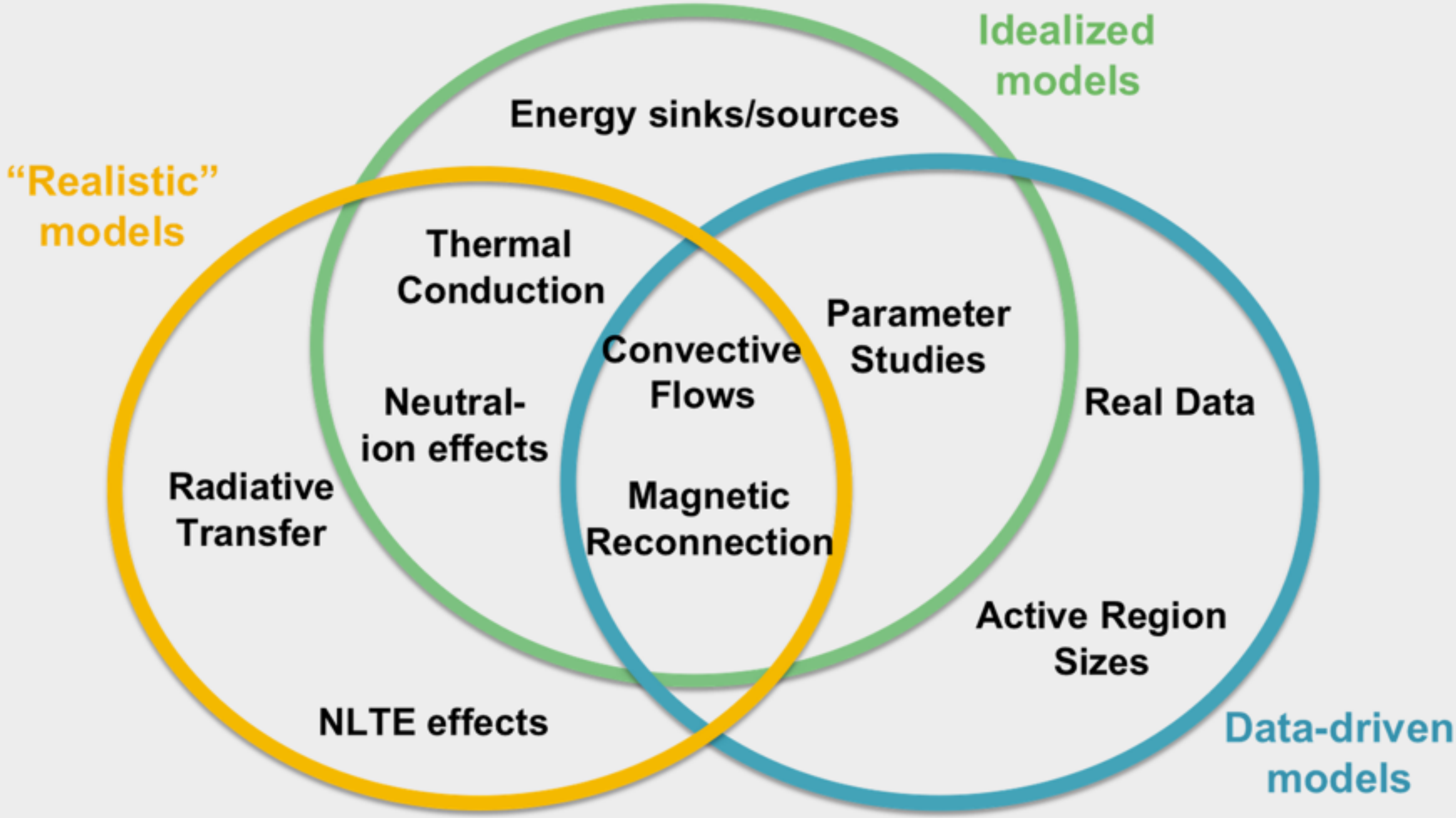

Figure 5: Models of magnetic flux emergence can be roughly divided into three categories, though there are large areas of overlap between them. So-called 'realistic' models attempt to include all the known important physical ingredients, while idealize models generally focus on studying a more limited set of effects. For case studies of certain observed emerging flux studies, data-driven models are used.

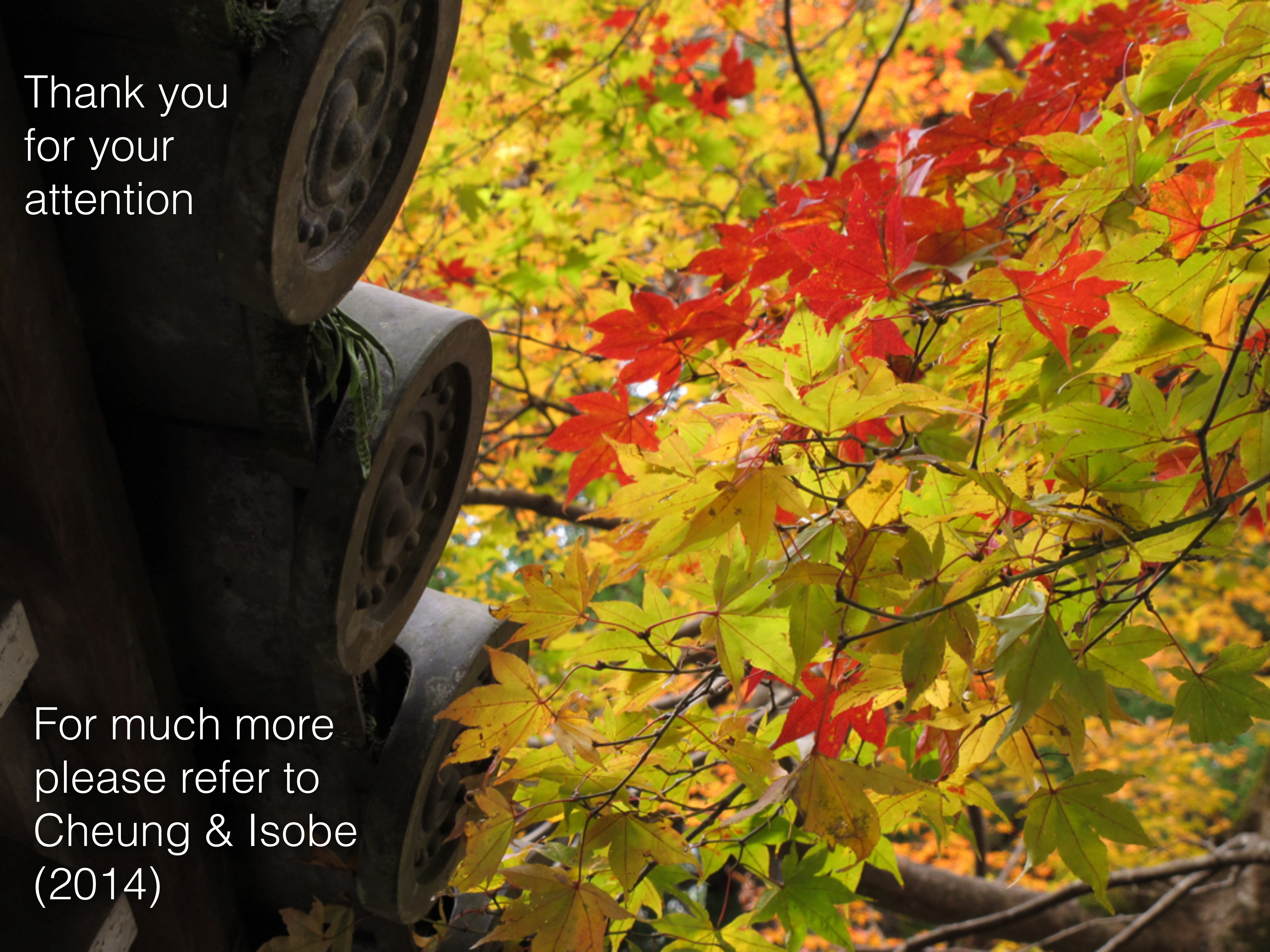
Thank you for your attention
For much more please refer to Cheung & Isobe (2014)